


Hippocampus Insulin Receptors Regulate Episodic and Spatial Memory Through Excitatory/Inhibitory Balance

Cai-Yan Xue^{1,†}, Tian Gao^{2,†}, E Mao³, Zhen-Zhen Kou³,
Ling Dong¹  and Feng Gao¹

ASN Neuro
Volume 15: 1–17
© The Author(s) 2023
Article reuse guidelines:
sagepub.com/journals-permissions
DOI: 10.1177/17590914231206657
journals.sagepub.com/home/asn



Abstract

It is well known that the hippocampus is a vital brain region playing a key role in both episodic and spatial memory. Insulin receptors (InsRs) are densely distributed in the hippocampus and are important for its function. However, the effects of InsRs on the function of the specific hippocampal cell types remain elusive. In this study, hippocampal InsRs knockout mice had impaired episodic and spatial memory. GABAergic neurons and glutamatergic neurons in the hippocampus are involved in the balance between excitatory and inhibitory (E/I) states and participate in the processes of episodic and spatial memory. InsRs are located mainly at excitatory neurons in the hippocampus, whereas 8.5% of InsRs are glutamic acid decarboxylase 2 (GAD2)::Ai9-positive (GABAergic) neurons. Next, we constructed a transgenic mouse system in which InsR expression was deleted from GABAergic (glutamate decarboxylase 2::InsR^{fl/fl}, GAD2^{Cre}::InsR^{fl/fl}) or glutamatergic neurons (vesicular glutamate transporter 2::InsR^{fl/fl}, Vglut2^{Cre}::InsR^{fl/fl}). Our results showed that in comparison to the InsR^{fl/fl} mice, both episodic and spatial memory were lower in GAD2^{Cre}::InsR^{fl/fl} and Vglut2^{Cre}::InsR^{fl/fl}. In addition, both GAD2^{Cre}::InsR^{fl/fl} and Vglut2^{Cre}::InsR^{fl/fl} were associated with more anxiety and lower glucose tolerance. These findings reveal that hippocampal InsRs might be crucial for episodic and spatial memory through E/I balance hippocampal regulation.

Keywords

hippocampus, insulin receptors, episodic memory, spatial memory, GABAergic neurons, glutamatergic neurons

Received June 30, 2023; Revised August 25, 2023; Accepted for publication September 23, 2023

Introduction

The hippocampus is a crucial region involved in memory, navigation, and cognition (Lisman et al., 2017). It is widely accepted that the hippocampus is essential for spatial memory processes, including the representation of environments (Dombeck et al., 2010) and episodic memory, which involves the ability to recall specific events (Burgess et al., 2002; Rangel et al., 2014). Spatial memory refers to the acquisition, storage and retrieval of information regarding the location of objects, as well as the recognition of changes in their positions within a given space (Llana et al., 2022). Episodic memory reflects the integration of different information recalling past experiences, such as time, place, and objects (Yonelinas et al., 2019).

Insulin receptors (InsRs) are characterized by high protein and gene expression in the pyramidal layer of the hippocampus (Havrankova et al., 1978; Marks et al., 1990; Unger et al., 1989). The structure and function of synapses are the basis of learning and memory formation (Mansvelder et al., 2019).

Previous studies have shown a strong association among InsRs, synaptic neuroplasticity, and episodic and spatial memory (Castellano et al., 2017; Masmudi-Martin et al.,

¹Key Laboratory of Aerospace Medicine of the Ministry of Education, School of Aerospace Medicine, Fourth Military Medical University, Xi'an, China

²Division of Health Management, Tangdu Hospital, Fourth Military Medical University, Xi'an, China

³Department of Anatomy, Histology and Embryology & K. K. Leung Brain Research Centre, Fourth Military Medical University, Xi'an, China

[†]These authors contributed equally.

Corresponding Author:

Zhen-Zhen Kou, School of Basic Medicine, Fourth Military Medical University, 169 Changle west Road, Xi'an 710032, China.
Email: plutoming@fmmu.edu.cn

Ling Dong, School of Aerospace Medicine, Fourth Military Medical University, 169 Changle west Road, Xi'an 710032, China.
Email: dongling@fmmu.edu.cn



2019). Therefore, InsRs might play a role in hippocampal episodic and spatial memory. However, little is known about the exact function of the specific cell types of InsRs in the hippocampus, particularly regarding their involvement in the processes of episodic and spatial memory.

The function of hippocampal network relies on a powerful excitatory glutamatergic system that is tightly controlled by inhibitory γ -aminobutyric acidergic (GABAergic) inhibition (Rombo et al., 2016). Importantly, the balance between excitability (E) and inhibition (I) is the basis of cognitive function (Mueller-Buehl et al., 2023). Two subtypes of neurons, the GABAergic and glutamatergic neurons play important roles in maintaining E/I balance. A healthy E/I balance promotes hippocampal spatial memory. On the contrary, disruptions in this balance impair synaptic plasticity and reduce synaptic number and function, resulting in learning function impairment (Lin et al., 2022; Mossink et al., 2022). Therefore, the maintenance of E/I balance by both GABAergic neurons and glutamatergic neurons may be involved in hippocampal episodic memory and spatial memory.

In this study, based on these considerations, we hypothesized that InsRs might participate in the formation of episodic and spatial memory in the hippocampus through regulating E/I balance. We first specifically knocked out hippocampal InsRs in the $InsR^{fl/fl}$ mice. Next, the Cre-loxP system was utilized to selectively delete the InsRs gene from GABAergic or glutamatergic neurons in mice ($GAD2^{Cre}::InsR^{fl/fl}$ or $Vglut2^{Cre}::InsR^{fl/fl}$) to investigate the effects of InsRs on GABAergic or glutamatergic neurons on episodic and spatial memory in mice.

Materials and Methods

Animals

First, C57BL/6 mice and transgenic $InsR^{fl/fl}$ mice of either gender (weighing 20–35 g and aged 6–8 weeks) were used for determining the InsRs expression of $InsR^{fl/fl}$ mice by comparison with that of normal C57BL/6 mice. Then, 13 $InsR^{fl/fl}$ mice were used for exploring the effects of hippocampal knockout of InsRs. The $InsR^{fl/fl}$ mice were constructed in the Institute of Model Animals of Nanjing University entrusted by our research group (Fu et al., 2015). The institute inserted loxP at both ends of exon 4 of the mouse insulin receptor gene and obtained homozygous $InsR^{fl/fl}$ after hybridization.

Second, $GAD2$ -IRES-Cre, $Vglut2$ -IRES-Cre mice (purchased from Jackson Laboratory, RRID : IMSR_JAX : 028867, RRID : IMSR_JAX : 028863, stock numbers are 019022 and 016963) and $B6.Cg-Gt(ROSA)26Sor^{tm9(CAG-tdTomato)Hze/J}$ mice (Ai9, purchased from Jackson Laboratory, RRID : IMSR_JAX : 007909, stock number is 007909) of either gender (weighing 20–35 g and aged 8–12 weeks) were utilized to study the influence of selective InsRs knockout on glutamatergic or GABAergic neurons.

All mice were housed under a 12 h light/dark cycle with *ad libitum* food and water access. Animal care and use strictly

followed institutional guidelines and governmental regulations. All protocols to reduce the suffering of the animal from the surgical operation were performed in compliance with the Animal Care and Use Committees' recommendations (NO: IACUC-20230079).

Brain Stereotaxic Injection

To specific knockout InsRs in the hippocampus, the $InsR^{fl/fl}$ mice were injected with recombinant adeno-associated virus (rAAV)-mediated Cre expression fused with hSyn as promoter of broad-spectrum neurons and enhanced with green fluorescent protein (rAAV-hSyn-EGFP-CRE) into the bilateral hippocampus. The $InsR^{fl/fl}$ mice received injections with rAAV-hSyn-EGFP were used as controls (Table 1).

Thirteen $InsR^{fl/fl}$ mice of either gender aged 6–8 weeks were randomly divided into two groups before the experiment. The mice were anesthetized by intraperitoneal injection of pentobarbital sodium (40 mg/kg). After successful anesthesia, the head was fixed on the brain stereotaxic instrument (RWD Life Science, Shenzhen, China). According to the brain atlas of mice, the virus was injected into bilateral hippocampus at two separate sites for both sides. The injection coordinates were as follows: bilateral hippocampus: 1.70 mm posterior to bregma, 1.87 mm lateral from midline, and 1.90 mm below the surface of the skull; bilateral hippocampus: 2.80 mm posterior to bregma, 3.10 mm lateral from midline, 3.45 mm below the surface of skull. By connecting the glass microtubule of a 1- μ L Hamilton microsyringe (Hamilton Company, Reno, NV, USA), the glass microelectrode was loaded with the virus (0.3 μ L) and pushed vertically and slowly to the target area through the foramen of the skull at a speed of 0.05 μ L/min. After the injection of the current site, the needle was left 15 min in the original position. After the virus has fully spread, quickly withdraw from the glass microelectrode to prevent the virus from leaking along the needle path as previously reported (Li et al., 2021).

Brain Slice Preparation

After deep anesthesia induced by pentobarbital sodium (40 mg/kg), mice of either gender for C57BL/6, $InsR^{fl/fl}$ mice, $InsR^{fl/fl}$, $GAD2^{Cre}::InsR^{fl/fl}$, $Vglut2^{Cre}::InsR^{fl/fl}$ mice and $GAD2$ -Cre::Ai9 mice at an age from 8 to 12 weeks ($n=3$) were perfused as described in detail in our previous report (Wu et al., 2023).

During perfusion, 50 mL of 0.01 M phosphate-buffered saline (PBS, pH 7.4) was used to rinse the blood, followed by 200 mL of 4% paraformaldehyde in 0.1 M phosphate buffer (PB, pH 7.4) to fix the tissues. After perfusion, the brains were removed and placed in the 4% paraformaldehyde fixed solution for post-fixed 4–6 h. Then the brains were immersed into 30% sucrose dissolved in 0.1 M PB until they sunk to the bottom of the containers.

Each brain was cut into 30 μ m transverse free-floating sections and collected sequentially in a 6-well culture plate on a freezing microtome (Leica CM1950 Cryostat RRID:

Table 1. Viral Vectors Used for Anatomical or Behavioral Purposes.

Experimental purposes	Viral vectors	Target	Volume	Serotype	Serial number
Control	rAAV-hSyn-EGFP	Bilateral hippocampus	0.3 μ l	AAV2/9	9-156-K220406
InsR KO	rAAV-hSyn-EGFP-CRE	Bilateral hippocampus	0.3 μ l	AAV2/9	9-905-K210501

Note: Viral vectors rAAV-hSyn-EGFP-CRE and rAAV-hSyn-EGFP were provided by Wuhan Brain VTA Co, Ltd. KO, knockout.

SCR_018061, CM1950; Leica, Wetzlar, Germany). The hippocampal serial sections of all groups were prepared and subjected to immunofluorescence staining, whereas the rest of the slices were preserved in cryopreservation solution.

Immunofluorescence Staining

The sections prepared for immunofluorescence staining were blocked with blocking solution (0.3% Triton X-100 and 5% donkey serum in 0.01 M PBS) for 1 h at room temperature and then incubated for three days at 4 °C with primary antibodies, including rabbit anti-insulin receptor (Abcam Cat# ab5500, RRID:AB_2296149, Abcam, 1:200), rabbit anti-CaMK II (Abcam Cat# ab134041, RRID:AB_2811181, Abcam, 1:600), mouse anti-synapsin Ia/b (Santa Cruz Biotechnology Cat# sc-376623, RRID:AB_11150313, Santa Cruz, 1:50), and mouse anti-NeuN (Sigma-Aldrich Cat# MAB377, RRID:AB_2298772, Millipore, 1:500).

After three-fold washing with 0.01 M PBS, the sections were incubated for one day at 4 °C with secondary antisera, including Alexa 594 donkey anti-mouse (Thermo Fisher Scientific Cat# A-21203, RRID:AB_141633, CA, 1:500), Alexa 488 donkey anti-rabbit (Thermo Fisher Scientific Cat# A-21206, RRID:AB_2535792, Invitrogen, CA, 1:500), and Alexa 647 donkey anti-mouse (Thermo Fisher Scientific Cat# A-31571, RRID:AB_162542, Invitrogen, CA, 1:500).

Finally, the sections were rinsed with PBS three times, mounted onto clean glass slides, and covered with fluorescent sealing mixture of 0.05 M PBS containing 50% (v/v) glycerin and 2.5% (w/v) triethylenediamine (Kou et al., 2013). The slices are observed and imaged under a confocal microscope (Zeiss LSM 780 Confocal Laser Scanning Microscope RRID:SCR_020922, Germany). The quantitative statistics of immunofluorescence staining were examined by ImageJ (RRID:SCR_003070) software. Quantitative analysis was performed by counting the number of immunopositive neurons from ten randomly selected three regions of hippocampus within 10 sections for each group of mice as specified in our previous publication (Kou et al., 2011).

Western Blotting

After deep anesthesia by pentobarbital sodium, six mice of either gender in each group (C57BL/6 and InsR^{fl/fl}), aged 6–8 weeks, were quickly decapitated, and the whole brains were removed on ice. The brains of the mice were next cut into two parts (left and right part). The left part was used as a brain sample for the subsequent detections. The cortex,

cerebellum, and hippocampus were anatomically carefully dissected from the right half.

Tissues from three C57BL/6 and three InsR^{fl/fl} mice were prepared and subjected to Western blotting. RT-qPCR tests were performed in the other three C57BL/6 and three InsR^{fl/fl} mice. The hippocampus of the mice in the InsR^{fl/fl}, GAD2^{Cre::InsR^{fl/fl}}, and Vglut2^{Cre::InsR^{fl/fl}} groups ($n = 3$) were harvested by using a previously described protocol (Van Hoeymissen et al., 2020).

For Western blotting, the freshly removed tissues were lysed with RIPA lysis buffer (Beyotime Biotechnology Co., Ltd. P0013B) and PMSF (Beyotime Biotechnology Co., Ltd. ST2573-5 g, dilution into: 1:100). After full homogenization, the tissues were centrifuged at 12,000 r/min and 4 °C for 15 min. The supernatant was retained for protein detection and concentration quantification by a BCA protein quantitative kit (Beyotime Biotechnology Co., Ltd.) and an FLUOstar Omega automatic multi-function enzyme labeling instrument (BMG LABTECH, Germany). The protein was denatured by SDS-PAGE gel (Bausch Bioengineering Co., Ltd.) electrophoresis (Bio-Rad Experion Automated Electrophoresis System RRID:SCR_019691, 164B-5070 Electrophoresis Instrument, Bio-Rad Co., Ltd.). The upper gel electrophoresis voltage was 80 V and the time was 40 min; the lower gel electrophoresis voltage was 120 V and the time was 90 min. The constant voltage 100 V was used for transferring the protein to polyvinylidene fluoride (PVDF, Millipore, USA) membrane for 90 min.

The PVDF membranes were blocked 5% skim milk at room temperature for 1 h, followed by overnight incubation with primary antibodies at 4 °C: rabbit anti α -Tubulin (11H10) antibody (Cell Signaling Technology Cat# 2125, RRID:AB_2619646, Cell Signaling Technology, USA, 1:1000), rabbit anti InsR β (4B8) antibody (Cell Signaling Technology Cat# 3025, RRID:AB_2280448, USA, 1:1000), mouse anti-synapsin Ia/b antibody (Santa Cruz Biotechnology Cat# sc-376623, RRID:AB_11150313, Santa Cruz, 1:100). After cleaning with phosphate buffered saline with Tween 20 (PBST) three times, the membranes were incubated with the horseradish peroxidase-labeled second antibody, including goat anti-mouse IgG (H + L) secondary antibody, HRP (Thermo Fisher Scientific Cat# 31430, RRID:AB_228307, 1:2000), and goat anti-rabbit IgG (H + L) secondary antibody, HRP (Thermo Fisher Scientific Cat# 31460, RRID:AB_228341, 1:2000) for 1 h at room temperature. After PBST cleaning, the expressions of target protein were detected by an OmegaLumC Chemiluminescence Imaging system (Shanghai Shize Biotechnology Co., Ltd.) and analyzed the gray value of the band by ImageJ (RRID:SCR_003070)

software. The relative expression levels of target protein were calculated using tubulin as the reference protein.

RT-qPCR Analysis

The brain, cortex, cerebellum, and hippocampus tissues of C57BL/6 and *InsR^{fl/fl}* mice (three in each group of either gender, aged 6–8 weeks) were harvested and conserved in enzyme-free EP tube. The total RNA was extracted from the brain, cortex, cerebellum, and hippocampus of each mouse as specified in our previous report (Kou et al., 2011). Next, the concentrations and purity of RNA were determined (DS-11 Ultra-micro UV-vis spectrophotometer, USA, DeNovix company). Subsequently, the cDNA reverse transcription was performed (BioRad T100 Thermal Cycler RRID:SCR_021921, Bio-Rad, T100, USA). The gene expressions of *InsRs* were detected by SYBR Green fluorescence quantitative PCR and analyzed (Bio-Rad CFX384 Real-Time Detection System RRID:SCR_018057, Bio-Rad, CFX384 Touch, USA). The sequences of the primers are presented in Table 2.

Mouse tubulin gene was utilized as the internal reference gene and the $2^{-\Delta\Delta C_t}$ method was performed for the quantitative PCR detection system as our previous report (Kou et al., 2011). The relative expression levels of the target gene mRNA in each sample were calculated.

Behavioral Assays

Mice prepared for behavioral tests were habituated in the recording chambers for 30 min before the tests. All behavioral tests were carried out within 8:00 a.m.–12:00 a.m. All behavioral studies were performed under blind conditions.

Open Field Test. Open field test (OFT) was performed following the procedure described in the literature (Li et al., 2021). During the testing period, each mouse was allowed to move freely in the area ($50 \times 50 \times 40$ cm) for 15 min and videotaped. An automated analysis system was employed to quantify the total distance traveled, mean speed, distance, and the time spent in the central zone by each mouse. At the end of test, the apparatus was cleaned with 75% ethanol before the next mouse was tested.

Elevated Plus Maze Test. As described in our previous report (Wu et al., 2023), the elevated plus maze test (EPM) was made of a white Plexiglas apparatus consisting of two

opposing open arms (30×5 cm), two opposing closed arms (30×5 cm), and a central area (5×5 cm). The platform was placed 50 cm above the floor. During the test, each of the mice were placed alone in the central area of the maze and explored for 5 min. The time spent in the open arms was recorded by the automated analysis system. The area was swabbed with 75% ethanol during the interval time between each trial.

Novel Object Recognition Test (NOR). The novel object recognition test (NOR) task evaluates the rodents' ability to recognize a novel object in the environment, reflecting episodic memory ability (Da Cruz et al., 2020).

Briefly, two similar cylinders (A and B) of the identical volume ($4 \times 4 \times 5$ cm) were fixed at diagonal corner from the wall for 10 cm. In the training session, each mouse was allowed to explore the objects for 10 min. After the training, the mice were returned to their home cages, and the equipment was cleaned with 75% ethanol. After 1 h of the habituation session, the object (B) was used as an old object and replaced by a cube with a volume of $4 \times 4 \times 4$ cm as a new object (C). Then, the mice were explored for another 10 min. After each test, cleaning and disinfection was performed before tests with the next mouse were initiated.

Morris Water Maze Test. The Morris water maze test (MWM) test was adopted for the evaluation of spatial cognitive performance in the mice. The apparatus utilized and the procedure of the water maze performed were described earlier (Fan et al., 2022). The water maze (diameter: 150 cm; height: 60 cm) with four quadrants was filled with warm water (25°C) to the level of 1.5 cm over the objective platform.

Mice were trained with four trials daily for four days. For training, each mouse was put into water randomly in one quadrant. The latency to the platform was recorded (if the mouse found the platform within 1 min, it was allowed to stay on the platform for 5 s and then taken out; if the mouse could not find the platform within 1 min, it was guided for learning for 5–10 s). After each mouse finished the training, it was put into a cage after drying its fur using a suitable temperature of a hot dryer, and left to rest for at least 30 min. On the fifth day, the platform was removed to allow the mice to swim freely in the maze for 1 min; the total time spent in the platform quadrant and the crossing time were recorded.

Intraperitoneal Glucose Tolerance Test

The glucose tolerance of the mice was assessed by intraperitoneal glucose tolerance test (IPGTT). Before the test, all mice were fasted for 16 h. At the baseline, the fasting blood glucose was recorded. The 20% glucose aqueous solution was injected intraperitoneally (2 g/kg, body weight) at 0 min. Then the blood glucose levels were measured (LifeScan, USA) at 15, 30, 90, and 120 min, respectively. The data were recorded and analyzed.

Table 2. Primer Sequences for RT-qPCR.

Primer	Primer sequence (5'-3')	
InsR	Upstream	GGATGTCCATACCAGGGCAC
	Downstream	ATGGGCTTCGGGAGAGGAT
Tubulin	Upstream	GATGACCTCCCAGAACTTGGC
	Downstream	TTTCGTCTCTAGCCGCGTG

Analyses

All behavioral tests, including OFT, NOR, EPM, and MWM, were analyzed by the relevant behavioral software (Smartsuper, Spain).

The relevant brain sections were observed by LSM780 laser confocal microscope (ZEISS, Germany) and the images were collected and analyzed by ImageJ.

All the experimental data were analyzed by Prism 8.0 software. The *t*-test was used to compare the two groups; the one-way analysis of variance (one-way ANOVA) was used to compare the three groups; the two-way analysis of variance (two-way ANOVA) was used to compare the escape latency of the MWM. The error bars represent standard error of mean (SEM). $p < .05$ was considered to indicate a statistically significant difference, $p > .05$ was considered to indicate a statistically non-significant difference.

Results

No Difference was Found in the Expression and Distribution of InsRs Between the InsR^{fl/fl} and C57BL/6 Mice

First, we aimed to determine whether the expression of InsRs in the brain of InsR^{fl/fl} mice was different from that in the brain of the C57BL/6 mice. Thus, the whole brain, cortex, cerebellum, and hippocampus were sampled from C57BL/6 and InsR^{fl/fl} mice. Western blotting, immunofluorescence staining, and RT-qPCR were implemented to detect the protein and mRNA levels of InsRs and to establish any differences between the two groups.

Western blotting results showed no significant differences in the expression levels of the InsRs protein in the whole brain, cortex, cerebellum, and hippocampus between the C57BL/6 and InsR^{fl/fl} mice (Figure 1A to C, C57BL/6 vs. InsR^{fl/fl}; brain, $p = .7831$; cortex, $p = .4989$; cerebellum, $p = .8338$; hippocampus, $p = .9998$). Compared with the C57BL/6 mice, there was no significant difference in the InsRs mRNA expression (Figure 1A and D, C57BL/6 vs. InsR^{fl/fl}; brain, $p = .9249$; cortex, $p = .9958$; cerebellum, $p = .8948$; hippocampus, $p = .9294$). We also conducted the double-labeled staining of InsR/NeuN to observe the distribution of InsR-immunoreactivities in the hippocampus. We found that InsR-positive elements were expressed similarly in the hippocampal areas of the two groups (Figure 1E).

These results indicated that there was no significant difference in the InsRs expression and distribution between C57BL/6 mice and InsR^{fl/fl} mice.

Construction of Hippocampal InsRs Knockout Mice

Since the expression of InsR in InsR^{fl/fl} mice are comparable to the C57BL/6 mice, next we sought to evaluate the relations between hippocampal InsRs knockout and episodic memory and spatial memory. The rAAV-hSyn-EGFP-CRE was stereotactically injected into the bilateral hippocampus of InsR^{fl/fl}

mice as hippocampal InsRs knockout, and the injection of rAAV-hSyn-EGFP in InsR^{fl/fl} mice was used as the control group (Figure 2A and B). The injection sites are displayed in Figure 2C.

The knockout efficiency was verified by Western blotting (Figure 2D). The expression of InsRs decreased significantly in the hippocampus rAAV-hSyn-EGFP-CRE group (Figure 2D and E, rAAV-hSyn-EGFP vs. rAAV-hSyn-EGFP-CRE, $p = .0239$, $n = 3$). Thus, using stereotaxic approaches, we were able to significantly reduce the InsRs expression in the hippocampus.

We also employed IPGTT to assess whether the hippocampal knockout of InsRs affected the peripheral glucose tolerance. Our results showed no significant difference in the area under curve, suggesting that peripheral glucose tolerance was unaffected in the mice with knockout of InsRs in the hippocampus (Figure 2F and G, rAAV-hSyn-EGFP vs. rAAV-hSyn-EGFP-CRE, area under curve: $p = .4400$, $n = 3$).

Behavioral Results of Hippocampal InsRs Knockout Mice

The Hippocampal InsRs Knockout Mice had Locomotor Ability and Emotional State Comparable to Those of the Control Mice. The OFT test was used to evaluate the animals' locomotor ability and interests in exploring space (Figure 3). Representative diagrams of the motion trajectories of the two groups of mice are displayed in Figure 3B. The results showed no significant difference in the total distance (cm) and mean speed (cm/s) between the mice in the rAAV-hSyn-EGFP and rAAV-hSyn-EGFP-CRE groups (Figure 3C and D), suggesting that the locomotor activity was comparable.

The distance (cm) and time (s) in the central zone reflect the degrees to which the mice were interested in exploring space. The data obtained here indicated that the hippocampal InsRs knockout mice were normal as those of the controls (Figure 3E and F, rAAV-hSyn-EGFP vs. rAAV-hSyn-EGFP-CRE, total distance (cm): $p = .9649$; mean speed (cm/s): $p = .9643$; distance in the central zone (cm): $p = .9367$; time in the central zone (s): $p = .8330$; $n = 7$).

The EPM test was employed to detect the emotional state of the mice, which was particularly valuable for evaluating anxiety-like behaviors (Figure 3G). Representative diagrams of motion trajectories of two groups of mice are illustrated in Figure 3H. The results showed no difference in the percentage of residence time to enter the open arm or the close arm between the rAAV-hSyn-EGFP and the rAAV-hSyn-EGFP-CRE groups (Figure 3I and J, rAAV-hSyn-EGFP vs. rAAV-hSyn-EGFP-CRE, open arm retention time percentage (%): $p = .9001$; close-arm retention time percentage (%): $p = .9001$). No difference was observed in the times to enter the open arm or the close arm between the rAAV-hSyn-EGFP and the rAAV-hSyn-EGFP-CRE groups (Figure 3K and L, rAAV-hSyn-EGFP vs. rAAV-hSyn-EGFP-CRE, open-arm entry times percentage (%): $p = .5731$; close arm entry times percentage (%): $p = .5731$).

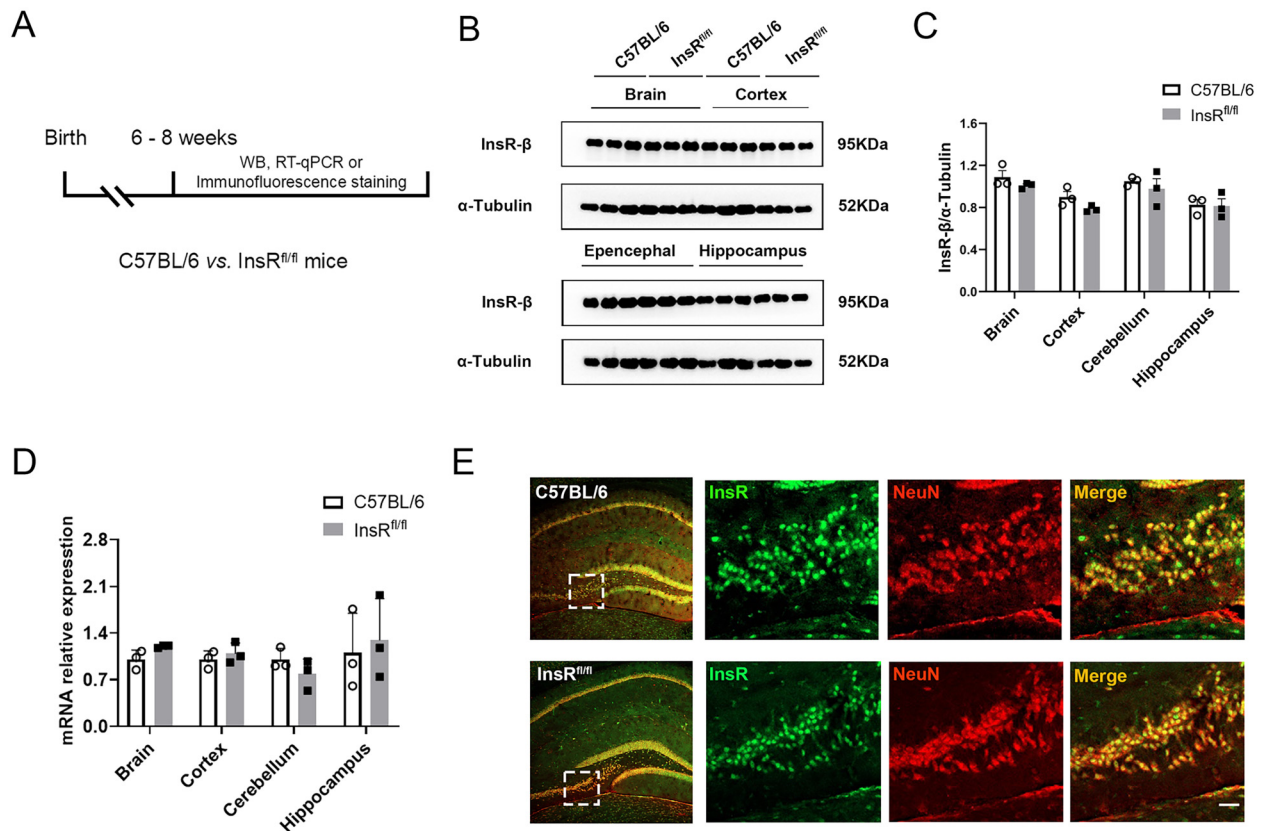


Figure 1. The differences in the InsRs expression between C57BL/6 and InsR^{fl/fl} mice were examined. (A) Schematic diagram of the study for comparison of InsR expression between C57BL/6 and InsR^{fl/fl} mice. (B) Representative Western blotting and analyses (C) of InsRs expressions in the brain, cortex, epencephala, hippocampus of C57BL/6 and InsR^{fl/fl} mice (paired *t*-test, *n* = 3). (D) RT-qPCR of C57BL/6 and InsR^{fl/fl} mice (paired *t*-test, *n* = 3). (E) Immunofluorescence staining for InsR and NeuN of the hippocampus of C57BL/6 and InsR^{fl/fl} mice. The values are expressed as mean ± SEM. Bar = 20 μm in E.

No obvious changes in the locomotor ability and emotional state of the hippocampal InsRs knockout mice were revealed by the results of the OFT and EPM experiments.

Hippocampal InsRs Knockout Mice Exhibit Impaired Episodic Memory and Spatial Memory. Further, we sought to evaluate the episodic memory and spatial memory of the hippocampal InsRs knockout mice. The NOR test was aimed to observe the episodic memory ability of mice. The results of the NOR test showed that the novel object discrimination index (%) of the rAAV-hSyn-EGFP-CRE group was lower than that of the rAAV-hSyn-EGFP group (Figure 4A to C, rAAV-hSyn-EGFP vs. rAAV-hSyn-EGFP-CRE, *p* = .0093, *n* = 6–7).

The MWM test was used to assess the spatial memory of mice (Figure 4D). Previous 4-day escape latency (s) results showed that the rAAV-hSyn-EGFP-CRE group always took longer time to find the platform location than the rAAV-hSyn-EGFP group (Figure 4E and F, rAAV-hSyn-EGFP vs. rAAV-hSyn-EGFP-CRE, 2-day: *p* = .0421; 3-day: *p* = .0409, *n* = 6–7). When the platform was removed, the time of rAAV-hSyn-EGFP-CRE group staying in the original platform area was less than that of

the rAAV-hSyn-EGFP group (Figure 4G, rAAV-hSyn-EGFP vs. rAAV-hSyn-EGFP-CRE, *p* = .0060, *n* = 6–7).

The results of NOR and MWM experiments showed the deficiency of episodic memory and spatial memory ability in the hippocampal InsRs knockout mice.

Distribution of CaMKII-Positive Excitatory, GABAergic Neurons, and InsR-Positive Neurons in the Hippocampus

To determine the expression of GABAergic or glutamatergic neurons in the hippocampus, specimens of the C57BL/6 mice and GAD2-Cre::Ai9 mice (the tdTomato sequence was knocked into the specific GAD2 site of GABAergic neurons, and the mice expressing red fluorescence in the central nervous system (CNS) were obtained as GAD2-Cre::Ai9 mice) were subjected to immunofluorescence staining.

The GABAergic neurons were observed in the hippocampus of mice (Figure 5C). For detecting the

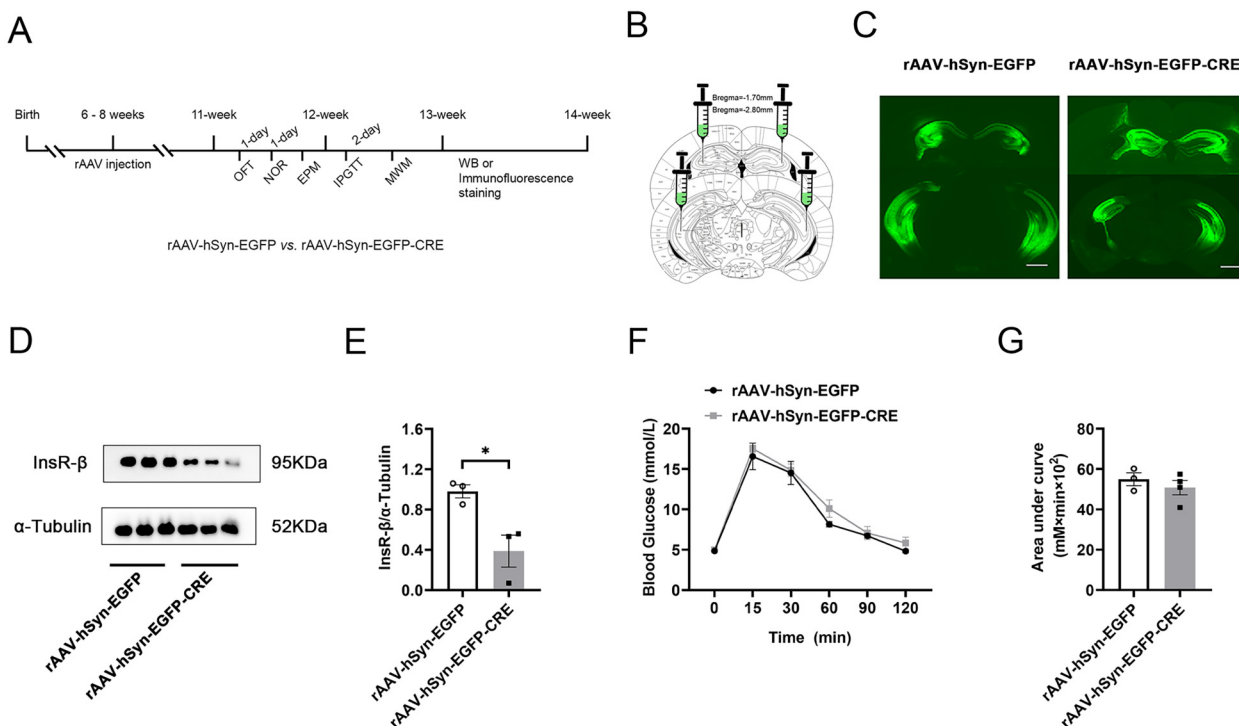


Figure 2. Construction of hippocampal InsRs knockout mice. (A) Schematic diagram of the strategy to knockout InsR in the hippocampus of InsR^{fl/fl} mice. (B) Schematic diagram showing injection sites of the rAAV-hSyn-EGFP and rAAV-hSyn-EGFP-CRE into bilateral hippocampus. (C) Representative images of rAAV-hSyn-EGFP and rAAV-hSyn-EGFP-CRE expression in the bilateral hippocampus after injection for three weeks. (D) Comparison of the InsR expression in the hippocampus of InsR^{fl/fl} mice injected with rAAV-hSyn-EGFP and rAAV-hSyn-EGFP-CRE in the Western blotting test (paired *t*-test, *n* = 3). (E) Analysis of the gray value of the band of InsR from Western blotting in the hippocampus of InsR^{fl/fl} mice injected with rAAV-hSyn-EGFP and rAAV-hSyn-EGFP-CRE (paired *t*-test, *n* = 3). (F) IPGTT curve of InsR^{fl/fl} mice injected with rAAV-hSyn-EGFP and rAAV-hSyn-EGFP-CRE (two-way ANOVA, *n* = 3–4). (G) The area under the IPGTT curve of InsR^{fl/fl} mice injected with rAAV-hSyn-EGFP and rAAV-hSyn-EGFP-CRE (unpaired *t*-test, *n* = 3–4). The values are expressed as mean \pm SEM, **p* < .05. Bar = 1 mm in C.

distribution pattern of the GAD2-positive GABAergic neurons in the hippocampus, we carried out immunohistochemistry analysis for GAD2-Cre::Ai9/NeuN/InsR. The obtained data indicated that GABAergic neurons were rarely distributed in the hippocampus (Figure 5C and D, 251/2497, 10.1%).

CaMKII is the most abundant protein in excitatory neurons and synapses, affecting synaptic plasticity, learning, and memory (Tao et al., 2021) in the hippocampus. The double-labeled immunohistochemistry results for CaMKII/NeuN indicate that glutamatergic neurons are widely distributed in the hippocampus, which is in accordance with previous report (Figure 5C and D, 1828/2211, 82.7%).

Immunohistochemistry results demonstrated that InsR/GABA-positive neurons were account for 8.5% (204/2408) of InsR-positive neurons in the hippocampus (Figure 5C and D).

Taken together, these results showed that glutamatergic neurons are highly expressed in the hippocampus than GABAergic neurons (Figure 5D, the ratios of GABA/NeuN vs. CaMKII/NeuN: 10.1%:82.7%).

The GAD2^{Cre}::InsR^{fl/fl} and Vglut2^{Cre}::InsR^{fl/fl} Transgenic Mice Showed Decreased InsRs Expression, Peripheral Glucose Tolerance and Hippocampal Synapsin Reduction

In order to further investigate the roles of InsRs in selective cell types of neurons in the hippocampus, we constructed transgenic mice with specific deletion of InsRs on GABAergic or glutamatergic neurons. In previous research of our team, we established a reliable homozygous InsR^{fl/fl} mice through the Cre-loxP system (Fu et al., 2015). Therefore, in the present study, we hybridized InsR^{fl/fl} mice with GAD2 or vesicular Vglut2 promoter-driven Cre recombinant enzyme to obtain the first generation GAD2^{Cre+/-}::InsR^{fl/-} or Vglut2^{Cre+/-}::InsR^{fl/-}, to backcross the InsR^{fl/fl} mice, resulting in homozygous second generation: GAD2^{Cre}::InsR^{fl/fl}, Vglut2^{Cre}::InsR^{fl/fl} mice or InsR^{fl/fl} for next investigations (Figure 5A).

The construction efficiency of transgenic mice was verified by Western blotting (Figure 5E). The results showed that InsRs in hippocampal GABAergic neurons or glutamatergic

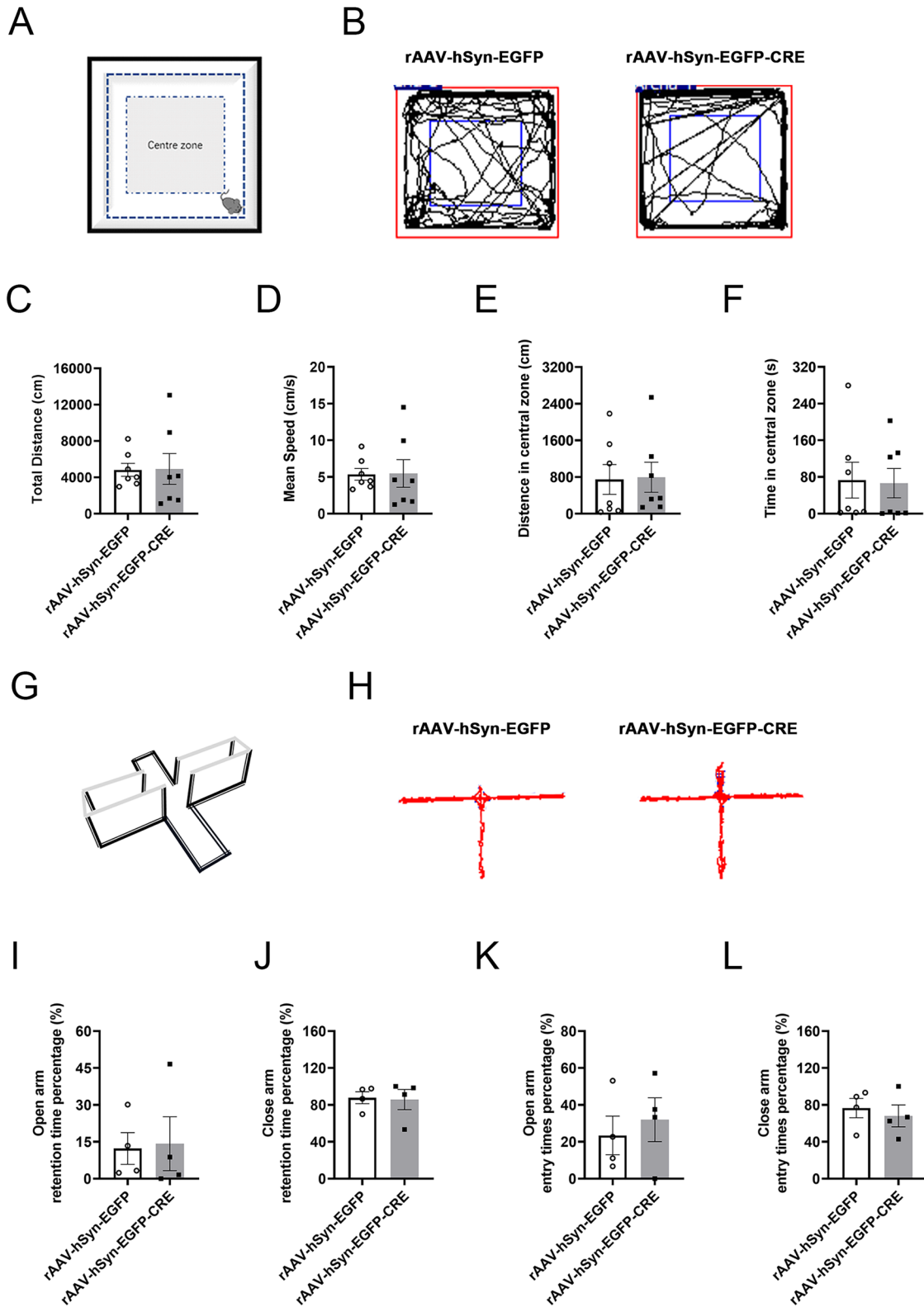


Figure 3. Locomotor activities and emotional changes in the OFT and EPM experiments of hippocampal InsR knockout mice. (A) Schematic diagram of the OFT test. (B) The representative trajectories in the OFT test of the rAAV-hSyn-EGFP and rAAV-hSyn-EGFP-CRE groups. (C) The total distance (cm), (D) mean speed (cm/s), (E) distance in the central zone (cm), (F) time in the central zone (s) of rAAV-hSyn-EGFP and rAAV-hSyn-EGFP-CRE groups (paired *t*-test, *n* = 7). (G) Schematic diagram of the EPM equipment. (H) The representative trajectories in the EPM of rAAV-hSyn-EGFP and rAAV-hSyn-EGFP-CRE groups. (I) Open arm retention time percentage (%), (J) close-arm retention time percentage (%), (K) open-arm entry times percentage (%), (L) close arm entry times percentage (%) of rAAV-hSyn-EGFP and rAAV-hSyn-EGFP-CRE groups (paired *t*-test, *n* = 4). The values are expressed as mean \pm SEM.

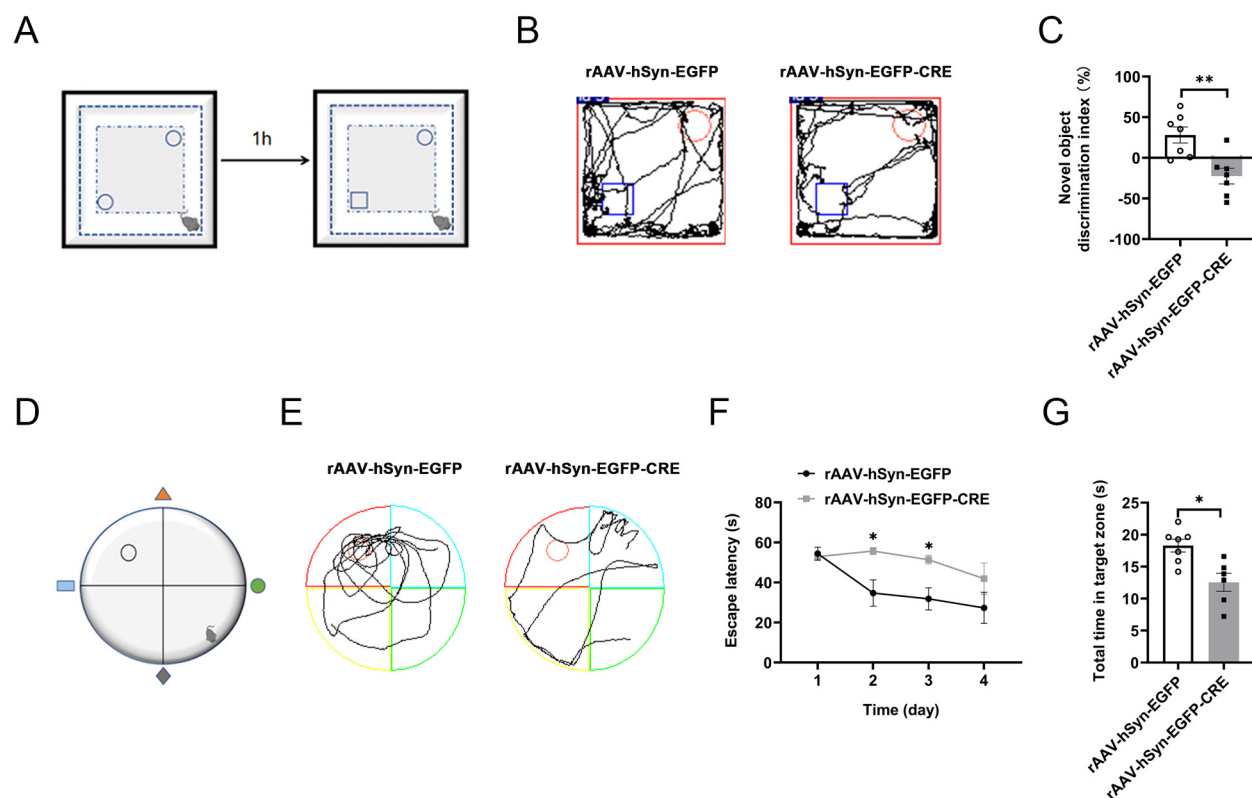


Figure 4. Alterations of the episodic memory and spatial memory ability in the NOR and MWM experiments of hippocampal InsR knockout mice. (A) Schematic diagram of the novel object recognition (NOR). (B) The NOR representative trajectories of rAAV-hSyn-EGFP and rAAV-hSyn-EGFP-CRE groups. (C) Novel object recognition discrimination index (%) of rAAV-hSyn-EGFP and rAAV-hSyn-EGFP-CRE groups (paired *t*-test, $n = 7$). (D) Schematic diagram of MWM. (E) The MWM representative trajectories diagrams of rAAV-hSyn-EGFP and rAAV-hSyn-EGFP-CRE groups during the test period. (F) Escape time (s) of rAAV-hSyn-EGFP and rAAV-hSyn-EGFP-CRE groups during the training period (two-way ANOVA, $n = 7$). (G) The total time in the target zone (s) of the rAAV-hSyn-EGFP and rAAV-hSyn-EGFP-CRE groups during the test period (unpaired *t*-test, $n = 6-7$). The values are expressed as mean \pm SEM, * $p < .05$, ** $p < .01$.

neurons mice were decreased (Figure 5F, InsR^{fl/fl} vs. GAD2^{Cre}::InsR^{fl/fl}, $p = .034$; InsR^{fl/fl} vs. Vglut2^{Cre}::InsR^{fl/fl}, $p = .0007$). Moreover, the InsR expression was more obviously diminished in the Vglut2^{Cre}::InsR^{fl/fl} than that of GAD2^{Cre}::InsR^{fl/fl} mice (Figure 5F, GAD2^{Cre}::InsR^{fl/fl} vs. Vglut2^{Cre}::InsR^{fl/fl}, $p = .0123$, $n = 3$), indicating that the InsRs on glutamatergic neurons accounted for higher proportion than GABAergic neurons in the mouse hippocampus.

Next, we aimed to establish whether this transgenic strategy influenced peripheral glucose tolerance. The IPGTT test results we obtained showed that after glucose injection, the levels of blood glucose in the GAD2^{Cre}::InsR^{fl/fl} and Vglut2^{Cre}::InsR^{fl/fl} mice were significantly higher when the InsR^{fl/fl} group was used as the control group, suggesting that the GAD2^{Cre}::InsR^{fl/fl} and Vglut2^{Cre}::InsR^{fl/fl} mice had higher glucose levels (Figure 5G and H, 15 min: InsR^{fl/fl} vs. GAD2^{Cre}::InsR^{fl/fl}, $p = .0005$; InsR^{fl/fl} vs. Vglut2^{Cre}::InsR^{fl/fl}, $p = .0148$; 30 min: InsR^{fl/fl} vs. GAD2^{Cre}::InsR^{fl/fl}, $p = .0001$; InsR^{fl/fl} vs. Vglut2^{Cre}::InsR^{fl/fl}, $p = .0486$; GAD2^{Cre}::InsR^{fl/fl} vs. Vglut2^{Cre}::InsR^{fl/fl}, $p = .0106$, $n = 5-8$). Furthermore, the results of the area under the curve showed that the peripheral glucose tolerance of the GAD2^{Cre}::InsR^{fl/fl} mice was

significantly lower (Figure 5H, InsR^{fl/fl} vs. GAD2^{Cre}::InsR^{fl/fl}, $p = .0039$; InsR^{fl/fl} vs. Vglut2^{Cre}::InsR^{fl/fl}, $p = .1944$; GAD2^{Cre}::InsR^{fl/fl} vs. Vglut2^{Cre}::InsR^{fl/fl}, $p = .1900$, $n = 5-8$).

Further, we explored the effects of InsRs reduction on hippocampal synapses. Previous evidence has revealed that the InsRs deletion specifically downregulates the expression of the glutamate receptor in synaptosomes from hippocampus, which is accompanied by multiple metabolic and behavioral abnormalities (Soto et al., 2019). Therefore, we further examined the effects of InsRs on hippocampal synapsin expression in both GAD2^{Cre}::InsR^{fl/fl} and Vglut2^{Cre}::InsR^{fl/fl} mice. Western blotting analysis revealed a decrease in synapsin expression in the hippocampus (Figure 6A and B, InsR^{fl/fl} vs. GAD2^{Cre}::InsR^{fl/fl}, $p = .0021$; InsR^{fl/fl} vs. Vglut2^{Cre}::InsR^{fl/fl}, $p = .0016$; GAD2^{Cre}::InsR^{fl/fl} vs. Vglut2^{Cre}::InsR^{fl/fl}, $p = .9616$, $n = 3$). This finding was further confirmed by an immunofluorescence staining experiment (Figure 6C and D). Reduced fluorescence intensity of synapsin in the hippocampus of the GAD2^{Cre}::InsR^{fl/fl} and Vglut2^{Cre}::InsR^{fl/fl} mice was observed (Figure 6D, InsR^{fl/fl} vs. GAD2^{Cre}::InsR^{fl/fl}, $p = .008$; InsR^{fl/fl} vs. Vglut2^{Cre}::InsR^{fl/fl}, $p = .0011$; GAD2^{Cre}::InsR^{fl/fl} vs. Vglut2^{Cre}::InsR^{fl/fl}, $p = .5110$, $n = 5$).

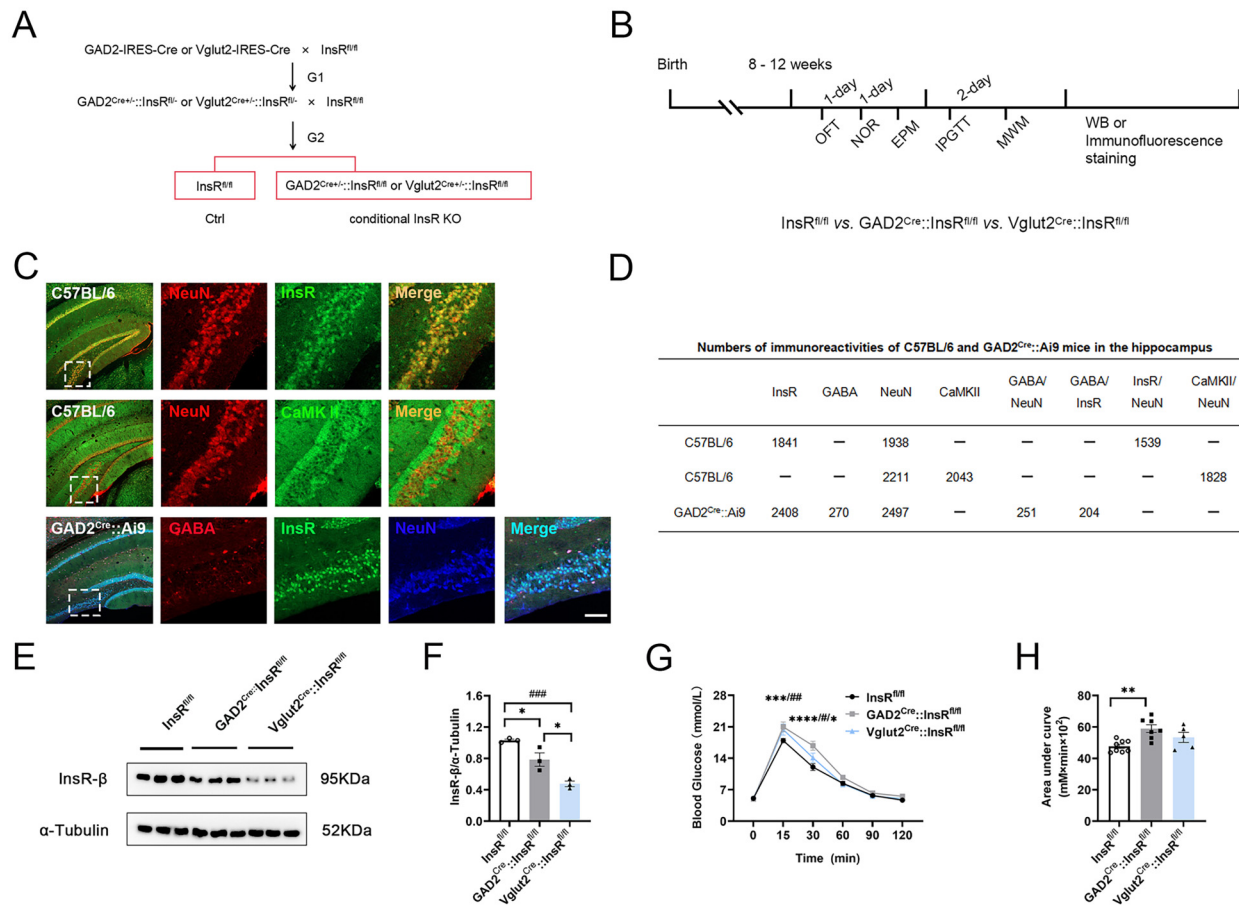


Figure 5. Changes in the specific knockout InsRs on GABAergic or glutamatergic neurons in GAD2^{Cre/+}::InsR^{fl/fl} and Vglut2^{Cre/+}::InsR^{fl/fl} transgenic mice, respectively. (A) Construction strategies of GAD2^{Cre/+}::InsR^{fl/fl} and Vglut2^{Cre/+}::InsR^{fl/fl} mice. (B) Schematic diagram of the strategy used to compare InsR^{fl/fl}, GAD2^{Cre/+}::InsR^{fl/fl} and Vglut2^{Cre/+}::InsR^{fl/fl} mice. (C) Immunofluorescence staining of C57BL/6 mice (CaMKII/NeuN and InsR/NeuN) and immunofluorescence staining of GAD2-Cre::Ai9 mice (GABA/InsR/NeuN). (D) Immunofluorescence staining analyses in the hippocampus of C57BL/6 and GAD2-Cre::Ai9 mice. (E) Western blotting of InsRs expression in the hippocampus of InsR^{fl/fl}, GAD2^{Cre/+}::InsR^{fl/fl} and Vglut2^{Cre/+}::InsR^{fl/fl} groups. (F) Western blotting analyses of InsRs expression of InsR^{fl/fl}, GAD2^{Cre/+}::InsR^{fl/fl} and Vglut2^{Cre/+}::InsR^{fl/fl} mice of the hippocampus (one-way ANOVA, $n = 3$). (G) The blood glucose levels with time in the IPGTT test of InsR^{fl/fl}, GAD2^{Cre/+}::InsR^{fl/fl} and Vglut2^{Cre/+}::InsR^{fl/fl} groups (two-way ANOVA, $n = 5-8$). (H) Area under of IPGTT curve of mice in the InsR^{fl/fl}, GAD2^{Cre/+}::InsR^{fl/fl} and Vglut2^{Cre/+}::InsR^{fl/fl} groups (one-way ANOVA, $n = 5-8$). The values are expressed as mean \pm SEM, * $p < .05$, ** $p < .01$, *** $p < .001$, InsR^{fl/fl} vs. GAD2^{Cre/+}::InsR^{fl/fl}, # $p < .05$, ### $p < .01$, #### $p < .001$, InsR^{fl/fl} vs. Vglut2^{Cre/+}::InsR^{fl/fl}. Bar = 20 μ m in C.

Taken together, these results suggested that the decreased InsRs might influence synapses, which are important for hippocampus function.

Behavioral Results of GAD2^{Cre/+}::InsR^{fl/fl} and Vglut2^{Cre/+}::InsR^{fl/fl} Mice

The GAD2^{Cre/+}::InsR^{fl/fl} and Vglut2^{Cre/+}::InsR^{fl/fl} Mice had Normal Locomotor Ability but Decreased Exploratory Behavior and Increased Anxiety. After the successful construction of the transgenic mice, OFT and EPM experiments were carried out. InsR^{fl/fl} mice were used as the control group. The results of OFT experiments showed no statistical difference in the comparisons of the InsR^{fl/fl}, GAD2^{Cre/+}::InsR^{fl/fl}, and

Vglut2^{Cre/+}::InsR^{fl/fl} mice in the total distance (cm) and mean speed (cm/s) (Figure 7A to C, total distance (cm): InsR^{fl/fl} vs. GAD2^{Cre/+}::InsR^{fl/fl}, $p = .0876$; InsR^{fl/fl} vs. Vglut2^{Cre/+}::InsR^{fl/fl}, $p = .0543$; GAD2^{Cre/+}::InsR^{fl/fl} vs. Vglut2^{Cre/+}::InsR^{fl/fl}, $p = .8913$; mean speed (cm/s): InsR^{fl/fl} vs. GAD2^{Cre/+}::InsR^{fl/fl}, $p = .0899$; InsR^{fl/fl} vs. Vglut2^{Cre/+}::InsR^{fl/fl}, $p = .0542$; GAD2^{Cre/+}::InsR^{fl/fl} vs. Vglut2^{Cre/+}::InsR^{fl/fl}, $p = .8850$, $n = 8-12$).

Importantly, the obtained data showed that the distance in the central zone and the time in the central zone of OFT were reduced in the GAD2^{Cre/+}::InsR^{fl/fl} and Vglut2^{Cre/+}::InsR^{fl/fl} groups, indicating that the mice had anxiety-like and reduced exploratory behaviors (Figure 7D and E, distance in the central zone (cm): InsR^{fl/fl} vs. GAD2^{Cre/+}::InsR^{fl/fl}, $p = .0401$; InsR^{fl/fl} vs. Vglut2^{Cre/+}::InsR^{fl/fl}, $p = .0037$; GAD2^{Cre/+}::InsR^{fl/fl} vs. Vglut2^{Cre/+}::InsR^{fl/fl}, $p = .4042$; time in

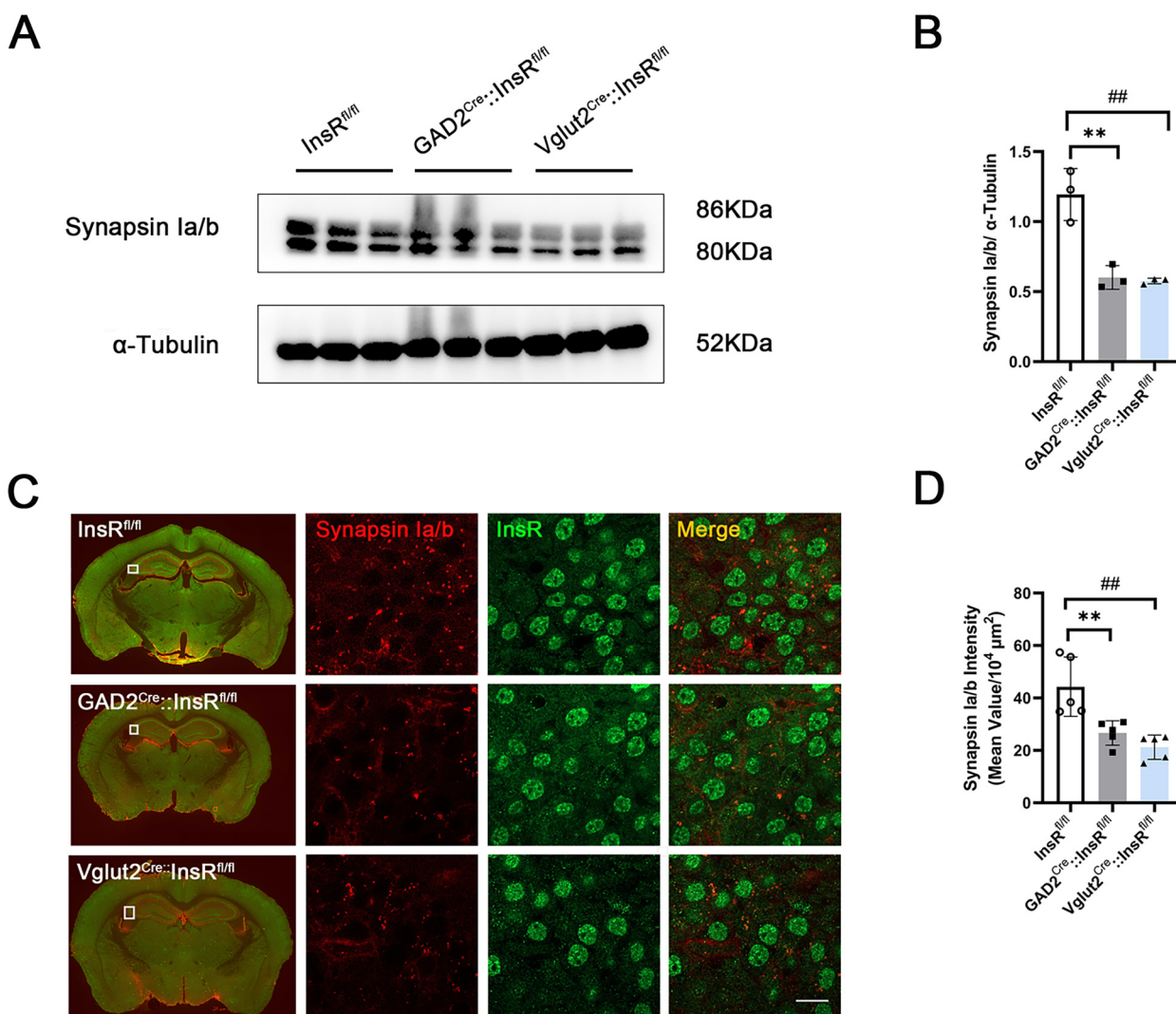


Figure 6. Changes in the hippocampal synapsin expression in the GAD2^{Cre}::InsR^{fl/fl} and Vglut2^{Cre}::InsR^{fl/fl} transgenic mice, respectively. (A) Western blotting results of synapsin Ia/b expression in the hippocampus of InsR^{fl/fl}, GAD2^{Cre}::InsR^{fl/fl} and Vglut2^{Cre}::InsR^{fl/fl} groups. (B) Analyses of the synapsin expression in the hippocampus of InsR^{fl/fl}, GAD2^{Cre}::InsR^{fl/fl} and Vglut2^{Cre}::InsR^{fl/fl} groups (one-way ANOVA, $n = 3$). (C) Immunofluorescence staining for Synapsin Ia/b and InsR in the InsR^{fl/fl}, GAD2^{Cre}::InsR^{fl/fl} and Vglut2^{Cre}::InsR^{fl/fl} mice. (D) Analyses of the fluorescence intensity of Synapsin Ia/b in the hippocampus of InsR^{fl/fl}, GAD2^{Cre}::InsR^{fl/fl} and Vglut2^{Cre}::InsR^{fl/fl} mice (one-way ANOVA, $n = 3$). The values are expressed as mean \pm SEM, * $p < .05$, ** $p < .01$, *** $p < .001$, InsR^{fl/fl} vs. GAD2^{Cre}::InsR^{fl/fl}, # $p < .05$, ## $p < .01$, #### $p < .001$, InsR^{fl/fl} vs. Vglut2^{Cre}::InsR^{fl/fl}. Bar = 50 μ m in C.

the central zone (s): InsR^{fl/fl} vs. GAD2^{Cre}::InsR^{fl/fl}, $p = .0326$; InsR^{fl/fl} vs. Vglut2^{Cre}::InsR^{fl/fl}, $p = .0230$; GAD2^{Cre}::InsR^{fl/fl} vs. Vglut2^{Cre}::InsR^{fl/fl}, $p = .9100$, $n = 8-12$).

According to the results of the EPM experiment, there were notable differences compared with the InsR^{fl/fl} group, percentage of the residence time in the open arm or the close arm of GAD2^{Cre}::InsR^{fl/fl} and Vglut2^{Cre}::InsR^{fl/fl}, suggesting the anxiety-like behaviors (Figure 7G and H, open arm retention time percentage (%): InsR^{fl/fl} vs. GAD2^{Cre}::InsR^{fl/fl}, $p = .0009$; InsR^{fl/fl} vs. Vglut2^{Cre}::InsR^{fl/fl}, $p = .0091$; GAD2^{Cre}::InsR^{fl/fl} vs. Vglut2^{Cre}::InsR^{fl/fl}, $p = .9050$; close-arm retention time percentage (%): InsR^{fl/fl} vs. GAD2^{Cre}::InsR^{fl/fl}, $p = .0025$;

InsR^{fl/fl} vs. Vglut2^{Cre}::InsR^{fl/fl}, $p = .0198$; GAD2^{Cre}::InsR^{fl/fl} vs. Vglut2^{Cre}::InsR^{fl/fl}, $p = .9138$, $n = 6-11$).

Similarly, the percentage of times to enter the open arm or the close arm of GAD2^{Cre}::InsR^{fl/fl} and Vglut2^{Cre}::InsR^{fl/fl} groups were prominent differences (Figure 7I and J, open-arm entry times percentage (%): InsR^{fl/fl} vs. GAD2^{Cre}::InsR^{fl/fl}, $p = .0032$; InsR^{fl/fl} vs. Vglut2^{Cre}::InsR^{fl/fl}, $p = .0422$; GAD2^{Cre}::InsR^{fl/fl} vs. Vglut2^{Cre}::InsR^{fl/fl}, $p = .6689$; close arm entry time percentage (%): InsR^{fl/fl} vs. GAD2^{Cre}::InsR^{fl/fl}, $p = .0032$; InsR^{fl/fl} vs. Vglut2^{Cre}::InsR^{fl/fl}, $p = .0422$; GAD2^{Cre}::InsR^{fl/fl} vs. Vglut2^{Cre}::InsR^{fl/fl}, $p = .6689$, $n = 6-11$).

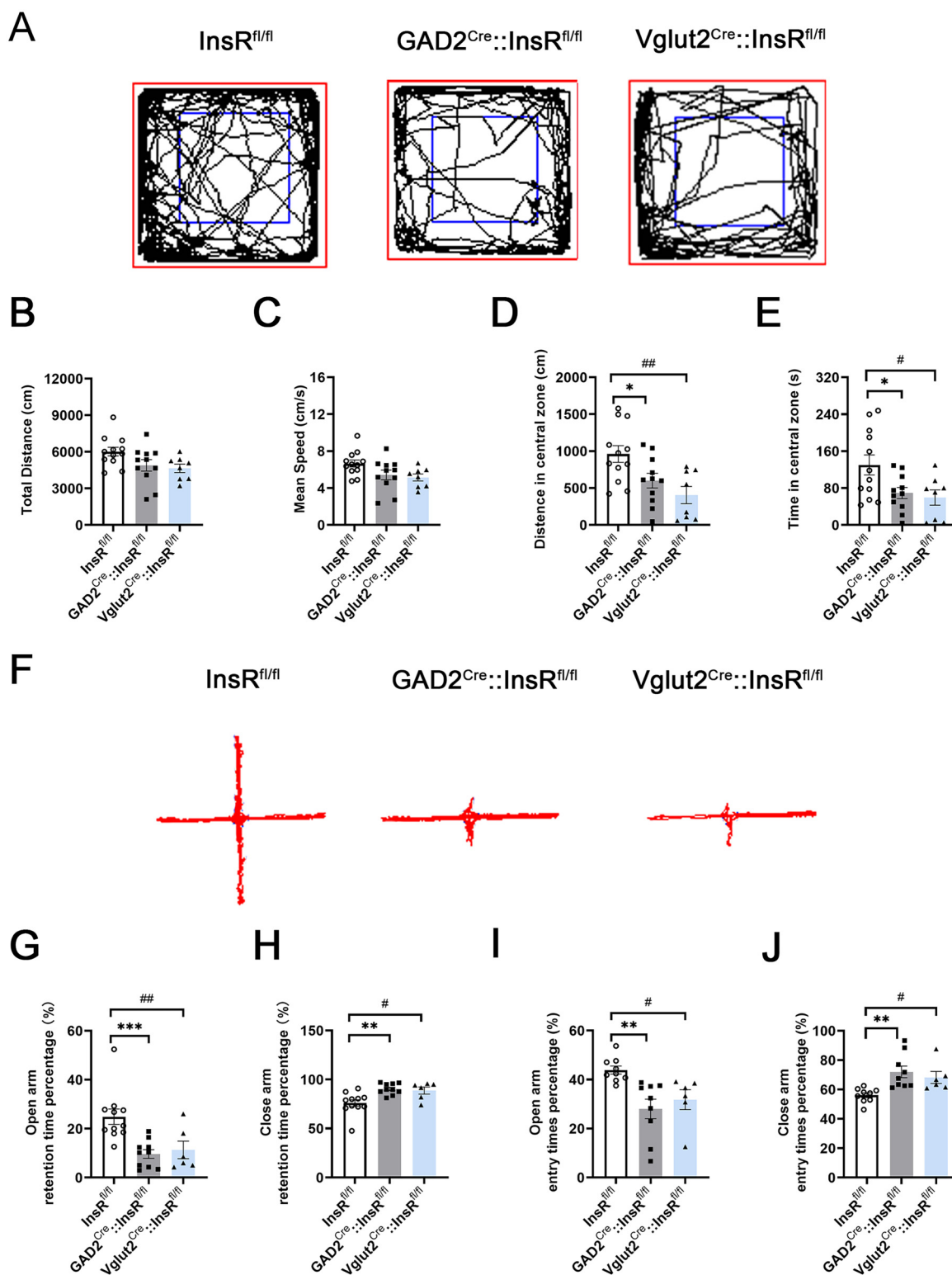


Figure 7. Locomotor activities and emotional changes in the OFT and EPM tests of $GAD2^{Cre::InsR^{fl/fl}}$ and $Vglut2^{Cre::InsR^{fl/fl}}$ mice. (A) The OFT representative trajectories of the $InsR^{fl/fl}$, $GAD2^{Cre::InsR^{fl/fl}}$ and $Vglut2^{Cre::InsR^{fl/fl}}$ groups (one-way ANOVA, $n = 8-12$). (B) The total distance (cm), (C) mean speed (cm/s), (D) distance in the central zone (cm), (E) time in the central zone (s) of $InsR^{fl/fl}$, $GAD2^{Cre::InsR^{fl/fl}}$ and $Vglut2^{Cre::InsR^{fl/fl}}$ groups. (F) The EPM representative trajectories of $InsR^{fl/fl}$, $GAD2^{Cre::InsR^{fl/fl}}$ and $Vglut2^{Cre::InsR^{fl/fl}}$ groups (one-way ANOVA, $n = 6-11$). (G) The open arm retention time percentage (%), (H) close-arm retention time percentage (%), (I) open-arm entry times percentage (%), (J) close-arm entry times percentage (%) of $InsR^{fl/fl}$, $GAD2^{Cre::InsR^{fl/fl}}$ and $Vglut2^{Cre::InsR^{fl/fl}}$ groups. The values are expressed as mean \pm SEM, * $p < .05$, ** $p < .01$, *** $p < .001$, $InsR^{fl/fl}$ vs. $GAD2^{Cre::InsR^{fl/fl}}$, # $p < .05$, ## $p < .01$, ### $p < .001$, $InsR^{fl/fl}$ vs. $Vglut2^{Cre::InsR^{fl/fl}}$.

Taken together, the results of OFT and EPM experiments revealed that the specific deletion of InsRs on the GABAergic or glutamatergic neurons of transgenic mice did not affect their locomotor performance but led to decreased exploratory behaviors and increased anxiety.

The $GAD2^{Cre}::InsR^{fl/fl}$ and $Vglut2^{Cre}::InsR^{fl/fl}$ Mice had Impaired Episodic and Spatial Memory. In the NOR tests, results indicated that the novel object discrimination index (%) of $GAD2^{Cre}::InsR^{fl/fl}$ and $Vglut2^{Cre}::InsR^{fl/fl}$ significantly lessened (Figure 8A and B, $InsR^{fl/fl}$ vs. $GAD2^{Cre}::InsR^{fl/fl}$, $p = .01$; $InsR^{fl/fl}$ vs. $Vglut2^{Cre}::InsR^{fl/fl}$, $p = .0004$; $GAD2^{Cre}::InsR^{fl/fl}$ vs. $Vglut2^{Cre}::InsR^{fl/fl}$, $p = .2326$, $n = 6-7$).

The escape latency (s) of the first 4-day period of the MWM showed that the mice needed a longer time to find the platform position for the $GAD2^{Cre}::InsR^{fl/fl}$ and $Vglut2^{Cre}::InsR^{fl/fl}$ mice (Figure 8C and D, 3-day: $InsR^{fl/fl}$ vs. $GAD2^{Cre}::InsR^{fl/fl}$, $p = .0033$; $InsR^{fl/fl}$ vs. $Vglut2^{Cre}::InsR^{fl/fl}$, $p = .1141$; 4-day: $InsR^{fl/fl}$ vs. $GAD2^{Cre}::InsR^{fl/fl}$, $p = .0099$; $InsR^{fl/fl}$ vs. $Vglut2^{Cre}::InsR^{fl/fl}$, $p = .0413$, $n = 5-7$). After the platform was removed on the test day, the time of both $GAD2^{Cre}::InsR^{fl/fl}$ and $Vglut2^{Cre}::InsR^{fl/fl}$ in the target area were significantly shorter than that of

the control group (Figure 8E, $InsR^{fl/fl}$ vs. $GAD2^{Cre}::InsR^{fl/fl}$, $p = .0152$; $InsR^{fl/fl}$ vs. $Vglut2^{Cre}::InsR^{fl/fl}$, $p = .0441$; $GAD2^{Cre}::InsR^{fl/fl}$ vs. $Vglut2^{Cre}::InsR^{fl/fl}$, $p = .09508$, $n = 5-7$).

Therefore, the behavioral results from both NOR and MWM tests indicated that the abilities of episodic memory and spatial memory were impaired in the transgenic mice with specific deletions of InsR on GABAergic neurons or glutamatergic neurons.

Discussion

Hippocampal InsRs Knockout Might Affect Mainly the Hippocampal Episodic and Spatial Memory

InsR is widely expressed in neurons in the hippocampus and have been shown to play a crucial role in the function of hippocampus (Hari Dass et al., 2019). In order to explore the specific role of InsRs in the hippocampus, we first established a mouse model of hippocampal InsRs knockout and assessed the performance in behavioral tests.

We found that knockout InsRs expression in the hippocampus resulted in impaired episodic and spatial memory. However, the OFT and EPM experiments showed that

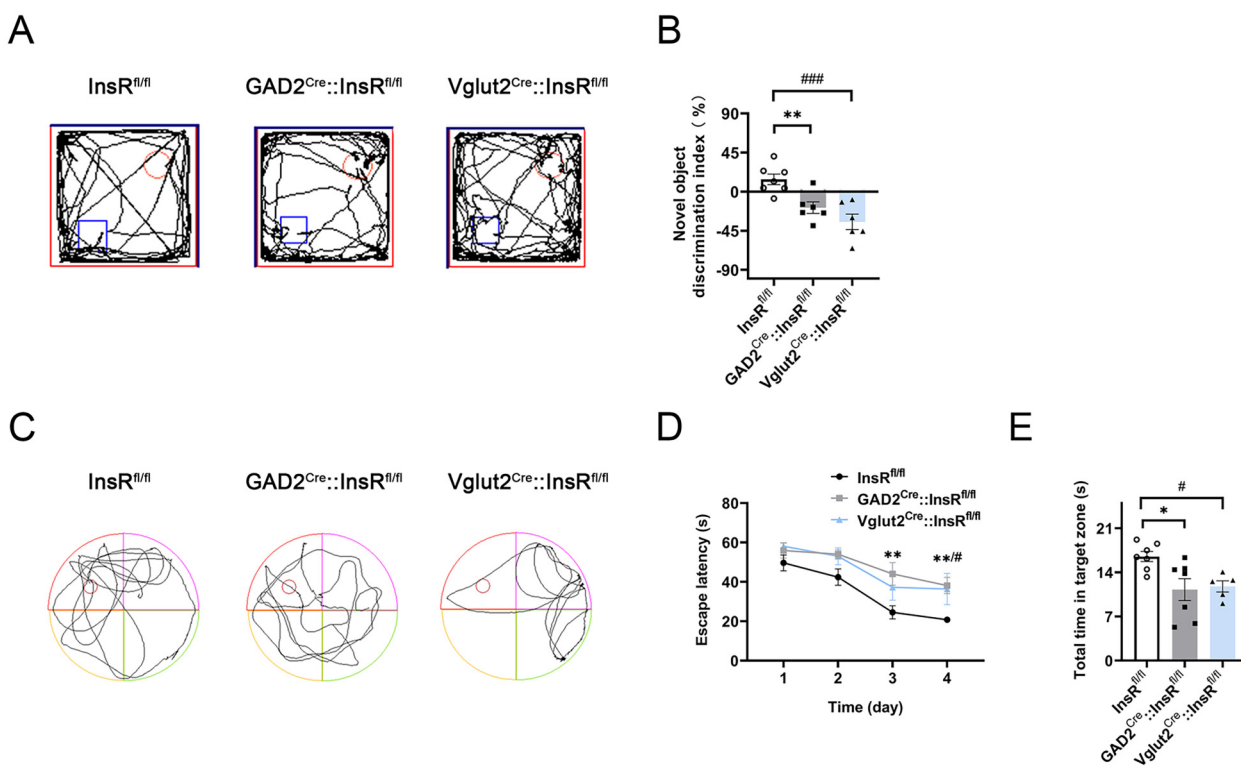


Figure 8. Alterations in the NOR and MWM experiments of $GAD2^{Cre}::InsR^{fl/fl}$ and $Vglut2^{Cre}::InsR^{fl/fl}$ mice. (A) The NOR representative trajectories of $InsR^{fl/fl}$, $GAD2^{Cre}::InsR^{fl/fl}$ and $Vglut2^{Cre}::InsR^{fl/fl}$ groups. (B) The novel object discrimination index (%) of $InsR^{fl/fl}$, $GAD2^{Cre}::InsR^{fl/fl}$ and $Vglut2^{Cre}::InsR^{fl/fl}$ groups (one-way ANOVA, $n = 6-7$). (C) The MWM representative trajectories of $InsR^{fl/fl}$, $GAD2^{Cre}::InsR^{fl/fl}$ and $Vglut2^{Cre}::InsR^{fl/fl}$ groups during the test period. (D) The escape time (s) of the $InsR^{fl/fl}$, $GAD2^{Cre}::InsR^{fl/fl}$ and $Vglut2^{Cre}::InsR^{fl/fl}$ groups during the training period (two-way ANOVA, $n = 5-7$). (E) The total time in the target zone (s) during the test period in the $InsR^{fl/fl}$, $GAD2^{Cre}::InsR^{fl/fl}$ and $Vglut2^{Cre}::InsR^{fl/fl}$ groups (one-way ANOVA, $n = 5-7$). The values are expressed as mean \pm SEM, * $p < .05$, ** $p < .01$, *** $p < .001$, $InsR^{fl/fl}$ vs. $GAD2^{Cre}::InsR^{fl/fl}$; # $p < .05$, ### $p < .01$, #### $p < .001$, $InsR^{fl/fl}$ vs. $Vglut2^{Cre}::InsR^{fl/fl}$.

Table 3. Summary of the Comparisons Among Different Group in InsRs Expression and Behavioral Results.

Analysis	C57BL/6	InsR ^{fl/fl}	InsR ^{fl/fl}		InsR ^{fl/fl} (Ctrl)	GAD2 ^{Cre} ::InsR ^{fl/fl}	Vglut2 ^{Cre} ::InsR ^{fl/fl}
			rAAV-hSyn-EGFP	rAAV-hSyn-EGFP-CRE			
WB—InsR-β	—	—	—	↓	—	↓	↓
WB—Synapsin Ia/b	—	—	—	—	—	↓	↓
RT-qPCR—InsR	—	—	—	—	—	—	—
Immunofluorescence staining—InsR	—	—	—	—	—	—	—
Immunofluorescence staining—Synapsin Ia/b	—	—	—	—	—	↓	↓
EPM	—	—	—	—	—	↓	↓
OFT-TD	—	—	—	—	—	—	—
OFT-MS	—	—	—	—	—	—	—
OFT-DICZ	—	—	—	—	—	↓	↓
OFT-TICZ	—	—	—	—	—	↓	↓
NOR	—	—	—	↓	—	↓	↓
IPGTT	—	—	—	—	—	↑	↑
MWM	—	—	—	↓	—	↓	↓

Note: “—”, no significant difference between groups. “↓”, significant decreased between groups. “↑”, significant increased between groups. Control, total distance, mean speed, distance in central zone and time in central zone are abbreviated as Ctrl, TD, MS, DICZ, TICZ, respectively.

hippocampal InsRs knockout mice did not exhibit anxiety and reduced exploratory behaviors. These results indicate that hippocampal InsRs play an important role mainly in episodic and spatial memory.

InsRs on GABAergic Neurons and Glutamatergic Neurons Might be Involved in the Episodic and Spatial Memory in the Hippocampus Through E/I Balance

An earlier study has shown that excitatory glutamatergic neurons are widely distributed in the hippocampus (Di Maio, 2021). The initiation of memory coding and the formation of learning and memory acts through the long-term enhancement of glutamatergic transmission (Cervera-Ferri et al., 2012). In a recent study, after targeted deletion of InsRs from the hippocampus of mice, the learning and memory-related impaired behaviors were combined with decreased expression of the excitatory glutamate receptor in the hippocampus (Soto et al., 2019). Interestingly, our results revealed that the knockout of InsRs in the glutamatergic neurons of Vglut2^{Cre}::InsR^{fl/fl} mice led to significant deficiencies in episodic and spatial memory. Based on the above results, it can be speculated that InsRs on glutamatergic neurons may be involved in regulating episodic and spatial memory in the hippocampus.

Notably, glutamatergic neurons in the hippocampus are outnumbered by GABAergic neurons (Pelkey et al., 2017). Despite their lower quantity, GABAergic neurons are essential in regulating local inhibition and E/I balance maintenance (Bhattacharya et al., 2022). Moreover, GABAergic inhibition is an important regulator of learning and memory potentiation (Davies et al., 1991), particularly in the hippocampus, where GABAergic neurons are also thought to encode spatial

information (Wilent & Nitz, 2007). In the present study, GABAergic neurons represented only 19% of the neurons in the hippocampus, which is consistent with previous reports (Kepecs & Fishell, 2014). However, the behavioral results showed that GAD2^{Cre}::InsR^{fl/fl} mice exhibited a significant decline in episodic memory and spatial memory as Vglut2^{Cre}::InsR^{fl/fl}, indicating that InsRs knockout on GABAergic neurons affected episodic and spatial memory.

Another important feature of hippocampal neural networks is the synaptic plasticity of neurons, which is the basis of memory-related processes in the hippocampus (Neves et al., 2008). InsRs present on the dendrites, soma, and axons of the hippocampal pyramidal cells could directly influence the synaptic plasticity and neurotransmitter release (Fetterly et al., 2021). For example, InsRs on GABAergic neurons can modify the GABA release and contribute to the regulation of hippocampal network (Hammoud et al., 2021). Our results showed that the expressions of synapsin of the hippocampus of GAD2^{Cre}::InsR^{fl/fl} and Vglut2^{Cre}::InsR^{fl/fl} mice decreased, suggesting that InsR deletions might affect the morphology and function of synapses. Nevertheless, further research is needed to clarify the precise mechanism in details.

The E/I balance is an important part of synaptic plasticity homeostasis. Studies have shown that the imbalance of E/I led to the defect in neurotransmitter release, postsynaptic receptors, and complexity of neural activity (Park et al., 2023). InsRs and downstream signaling pathway can directly participate in the regulation of glutamatergic neurons and GABAergic neurons. E/I balance was found to be disturbed in autism spectrum disorder (ASD) patients (Rubenstein & Merzenich, 2003). Interestingly, the potential mechanism of positive effect in ASD patients is the normalization of E/I balance by enhancing the InsRs signaling pathway (Lo & Erzurumlu, 2018).

Our results revealed that InsRs is distributed mainly in excitatory neurons, although it could also be observed in GABAergic neurons. Both $GAD^{Cre}::InsR^{fl/fl}$ and $Vglut2::InsR^{fl/fl}$ mice exhibited impaired episodic and spatial memory.

Therefore, InsRs might play an important role in both excitatory neurons and inhibitory neurons. The loss of InsRs on either GABAergic or glutamatergic neurons cannot ensure the preservation of episodic and spatial memory in the hippocampus. Both InsRs on the GABAergic neurons and glutamatergic neurons might be necessary for maintaining hippocampal episodic memory and spatial memory function by regulating E/I balance. Therefore, InsRs deficiency on either GABAergic or glutamatergic neurons might damage E/I balance, leading to impaired synaptic plasticity and network dynamics. Nonetheless, further research is required to clarify the exact mechanism of action.

Taken together, InsRs might play a vital role in maintaining the E/I balance in the hippocampal circuit by regulating the activity and interactions of GABAergic and glutamatergic neurons.

Effects of Deleting InsRs From GABAergic or Glutamatergic Neurons on Emotional State and Peripheral Glucose Metabolism

Interestingly, the deletion of InsRs from glutamatergic or GABAergic neurons seemed not to affect the locomotor ability of mice. However, there were statistical differences in the changes of animal anxiety-like and exploratory behaviors in the OFT and EPM experiments in both $GAD2^{Cre}::InsR^{fl/fl}$ and $Vglut2^{Cre}::InsR^{fl/fl}$ mice.

Comparing with hippocampal knockout InsRs mice, there was no significant anxiety-like and decreased exploratory behaviors, suggesting that the behavioral changes of specific hippocampal InsR knockout in $InsR^{fl/fl}$ mice were not fully consistent with the subtype-specific neuronal InsR deletions in $GAD^{Cre}::InsR^{fl/fl}$ or $Vglut2::InsR^{fl/fl}$ mice. This might be explained by the InsRs expressions in different regions. The results of a previous study also showed the widespread localization of InsRs in the hypothalamus (Grillo et al., 2011). These authors established that the downregulation of hypothalamic InsRs expression increased the anxiety-like behavior in rodents.

In the exploration of hippocampal InsR knockout, we injected rAAV-hSyn-EGFP-CRE to specifically delete the InsR in the hippocampus of the $InsR^{fl/fl}$ mice. Therefore, the changes in the results of the behavioral tests should be attributed to the deletions of InsRs in the hippocampus alone. However, in the $GAD^{Cre}::InsR^{fl/fl}$ and $Vglut2::InsR^{fl/fl}$ mice, except for hippocampal InsRs, other brain or spinal regions where GABAergic or glutamatergic neurons co-expressed with InsRs might also be influenced by knockout. In the present study, we focused mainly on investigations of the roles of InsRs in the hippocampus. As can be seen in Figures 4 and 8, in both the rAAV-hSyn-EGFP-CRE group and the $GAD^{Cre}::InsR^{fl/fl}$

group, $Vglut2::InsR^{fl/fl}$ mice had impaired episodic and spatial memory in our NOR and MWM tests.

In the IPGTT experiment, after the administration of a glucose injection, the glucose levels in the $GAD2^{Cre}::InsR^{fl/fl}$ and $Vglut2^{Cre}::InsR^{fl/fl}$ mice were higher than those in the $InsR^{fl/fl}$ mice. However, we did not observe a significant difference in the IPGTT results in mice with hippocampal InsRs knockout. This result suggests that the hippocampal specific downregulation of InsRs may not have an impact on peripheral glucose metabolism.

It is important to note that InsRs are widely distributed throughout the CNS and peripheral nervous system, especially in areas closely related to metabolism, such as the hypothalamic paraventricular nucleus (PVN) and the arcuate nucleus (Cassaglia et al., 2011; Chen et al., 2022). Earlier research has established the involvement of the hypothalamus in glucose metabolism; inhibitory GABAergic antagonists or excitability glutamatergic agonists in the PVN have been shown to induce hyperglycemia (Kalsbeek et al., 2008). Therefore, the differences between $GAD2^{Cre}::InsR^{fl/fl}$, $Vglut2^{Cre}::InsR^{fl/fl}$ mice, and hippocampal InsRs knockout mice in the IPGTT tests may be attributed to the fact that, InsR/GABA or InsR/Vglut2 co-expressed neurons are distributed not only in the hippocampus, but also in other areas related to glucose metabolism, which are involved in the regulation of peripheral blood glucose levels in $GAD2^{Cre}::InsR^{fl/fl}$ and $Vglut2^{Cre}::InsR^{fl/fl}$ mice.

While the present study has only suggested the role of InsRs in the hippocampal function, it is important to note that insulin may also act through the insulin-like growth factor receptor 1 (IGFR1) system in the hippocampus. Therefore, the underlying mechanism needs to be further studied.

Conclusions

The results of the present work showed that InsRs in the hippocampus are particularly important for episodic and spatial memory in mice. Furthermore, we also further investigated the effects of deficiency of InsRs on either GABAergic or glutamatergic neurons, leading to the E/I imbalance and impairments in episodic and spatial memory in the hippocampus. In addition, the absence of InsRs on GABAergic or glutamatergic neurons might result in emotional changes and increased peripheral glucose tolerance (Table 3).

Declaration of Conflicting Interests

The authors declared no potential conflicts of interest with respect to the research, authorship, and/or publication of this article.

Funding

The authors disclosed receipt of the following financial support for the research, authorship, and/or publication of this article: This work was supported by National Natural Science Foundation of China, Space Medical Experiment Project of China Manned Space Program, Shaanxi (grant number Nos. 81971035, 31971059, 81870273, HYZHXM01001, 2019SF-083).

ORCID iD

Ling Dong  <https://orcid.org/0000-0001-9960-6843>

References

- Bhattacharya, D., Bartley, A. F., Li, Q., & Dobrunz, L. E. (2022). Bicuculline restores frequency-dependent hippocampal I/E ratio and circuit function in PGC-1a null mice. *Neuroscience Research*, *184*, 9–18. <https://doi.org/10.1016/j.neures.2022.07.003>
- Burgess, N., Maguire, E. A., & O'Keefe, J. (2002). The human hippocampus and spatial and episodic memory. *Neuron*, *35*(4), 625–641. [https://doi.org/10.1016/S0896-6273\(02\)00830-9](https://doi.org/10.1016/S0896-6273(02)00830-9)
- Cassaglia, P. A., Hermes, S. M., Aicher, S. A., & Brooks, V. L. (2011). Insulin acts in the arcuate nucleus to increase lumbar sympathetic nerve activity and baroreflex function in rats. *Journal of Physiology*, *589*(7), 1643–1662. <https://doi.org/10.1113/jphysiol.2011.205575>
- Castellano, J. M., Mosher, K. I., Abbey, R. J., McBride, A. A., James, M. L., Berdnik, D., Shen, J. C., Zou, B., Xie, X. S., Tingle, M., Hinkson, I. V., Angst, M. S., & Wyss-Coray, T. (2017). Human umbilical cord plasma proteins revitalize hippocampal function in aged mice. *Nature*, *544*(7651), 488–492. <https://doi.org/10.1038/nature22067>
- Cervera-Ferri, A., Rahmani, Y., Martinez-Bellver, S., Teruel-Marti, V., & Martinez-Ricos, J. (2012). Glutamatergic projection from the nucleus incertus to the septohippocampal system. *Neuroscience Letters*, *517*(2), 71–76. <https://doi.org/10.1016/j.neulet.2012.04.014>
- Chen, W., Cai, W., Hoover, B., & Kahn, C. R. (2022). Insulin action in the brain: Cell types, circuits, and diseases. *Trends in Neurosciences*, *45*(5), 384–400. <https://doi.org/10.1016/j.tins.2022.03.001>
- Da Cruz, J. F. O., Gomis-Gonzalez, M., Maldonado, R., Marsicano, G., Ozaita, A., & Busquets-García, A. (2020). An alternative maze to assess novel object recognition in mice. *Bio-protocol*, *10*(12), e3651–e3651. <https://doi.org/10.21769/BioProtoc.3651>
- Davies, C. H., Starkey, S. J., Pozza, M. F., & Collingridge, G. L. (1991). GABA autoreceptors regulate the induction of LTP. *Nature*, *349*(6310), 609–611. <https://doi.org/10.1038/349609a0>
- Di Maio, V. (2021). The glutamatergic synapse: A complex machinery for information processing. *Cognitive Neurodynamics*, *15*(5), 757–781. <https://doi.org/10.1007/s11571-021-09679-w>
- Dombeck, D. A., Harvey, C. D., Tian, L., Looger, L. L., & Tank, D. W. (2010). Functional imaging of hippocampal place cells at cellular resolution during virtual navigation. *Nature Neuroscience*, *13*(11), 1433–1440. <https://doi.org/10.1038/nn.2648>
- Fan, Z., Liang, L., Ma, R., Xie, R., Zhao, Y., Zhang, M., Guo, B., Zeng, T., He, D., Zhao, X., & Zhang, H. (2022). Maternal sevoflurane exposure disrupts oligodendrocyte myelination of the postnatal hippocampus and induces cognitive and motor impairments in offspring. *Biochemical and Biophysical Research Communications*, *614*, 175–182. <https://doi.org/10.1016/j.bbrc.2022.05.037>
- Fetterly, T. L., Oginsky, M. F., Nieto, A. M., Alonso-Caraballo, Y., Santana-Rodriguez, Z., & Ferrario, C. R. (2021). Insulin bidirectionally alters NAc glutamatergic transmission: Interactions between insulin receptor activation, endogenous opioids, and glutamate release. *Journal of Neuroscience*, *41*(11), 2360–2372. <https://doi.org/10.1523/JNEUROSCI.3216-18.2021>
- Fu, F., Zhao, K., Li, J., Xu, J., Zhang, Y., Liu, C., Yang, W., Gao, C., Li, J., Zhang, H., Li, Y., Cui, Q., Wang, H., Tao, L., Wang, J., Quon, M. J., & Gao, F. (2015). Direct evidence that myocardial insulin resistance following myocardial ischemia contributes to post-ischemic heart failure. *Scientific Reports*, *5*(1), 17927–17927. <https://doi.org/10.1038/srep17927>
- Grillo, C. A., Piroli, G. G., Kaigler, K. F., Wilson, S. P., Wilson, M. A., & Reagan, L. P. (2011). Downregulation of hypothalamic insulin receptor expression elicits depressive-like behaviors in rats. *Behavioural Brain Research*, *222*(1), 230–235. <https://doi.org/10.1016/j.bbr.2011.03.052>
- Hammoud, H., Netsyk, O., Tafreshiha, A. S., Korol, S. V., Jin, Z., Li, J. P., & Birnir, B. (2021). Insulin differentially modulates GABA signalling in hippocampal neurons and, in an age-dependent manner, normalizes GABA-activated currents in the tg-APP^{Swe} mouse model of Alzheimer's disease. *Acta Physiologica (Oxf)*, *232*(2), e13623–e13623. <https://doi.org/10.1111/apha.13623>
- Hari Dass, S. A., McCracken, K., Pokhvisneva, I., Chen, L. M., Garg, E., Nguyen, T. T. T., Wang, Z., Barth, B., Yaqubi, M., McEwen, L. M., MacIsaac, J. L., Diorio, J., Kobor, M. S., O'Donnell, K. J., Meaney, M. J., & Silveira, P. P. (2019). A biologically-informed polygenic score identifies endophenotypes and clinical conditions associated with the insulin receptor function on specific brain regions. *EBioMedicine*, *42*, 188–202. <https://doi.org/10.1016/j.ebiom.2019.03.051>
- Havrankova, J., Roth, J., & Brownstein, M. (1978). Insulin receptors are widely distributed in the central nervous system of the rat. *Nature*, *272*(5656), 827–829. <https://doi.org/10.1038/272827a0>
- Kalsbeek, A., Foppen, E., Schalij, L., Van Heijningen, C., van der Vliet, J., Fliers, E., & Buijs, R. M. (2008). Circadian control of the daily plasma glucose rhythm: An interplay of GABA and glutamate. *PLoS One*, *3*(9), e3194–e3194. <https://doi.org/10.1371/journal.pone.0003194>
- Kepecs, A., & Fishell, G. (2014). Interneuron cell types are fit to function. *Nature*, *505*(7483), 318–326. <https://doi.org/10.1038/nature12983>
- Kou, Z. Z., Li, C. Y., Tang, J., Hu, J. C., Qu, J., Liao, Y. H., Wu, S. X., Li, H., & Li, Y. Q. (2013). Down-regulation of insulin signaling is involved in painful diabetic neuropathy in type 2 diabetes. *Pain Physician*, *16*, E71–E83.
- Kou, Z. Z., Zhang, Y., Zhang, T., Li, H., & Li, Y. Q. (2011). Age-related increase in PKC gamma expression in the cochlear nucleus of hearing impaired C57BL/6J and BALB/c mice. *Journal of Chemical Neuroanatomy*, *41*(1), 20–24. <https://doi.org/10.1016/j.jchemneu.2010.10.003>
- Li, J. N., Ren, J. H., He, C. B., Zhao, W. J., Li, H., Dong, Y. L., & Li, Y. Q. (2021). Projections from the lateral parabrachial nucleus to the lateral and ventral lateral periaqueductal gray subregions mediate the itching sensation. *Pain*, *162*(6), 1848–1863. <https://doi.org/10.1097/j.pain.0000000000002193>
- Lin, L., Zhang, J., Dai, X., Xiao, N., Ye, Q., & Chen, X. (2022). A moderate duration of stress promotes behavioral adaptation and spatial memory in young C57BL/6J mice. *Brain Sciences*, *12*(8), 1081. <https://doi.org/10.3390/brainsci12081081>
- Lisman, J., Buzsaki, G., Eichenbaum, H., Nadel, L., Ranganath, C., & Redish, A. D. (2017). Viewpoints: How the hippocampus contributes to memory, navigation and cognition. *Nature Neuroscience*, *20*(11), 1434–1447. <https://doi.org/10.1038/nn.4661>
- Llana, T., Fernandez-Baizán, C., Mendez-Lopez, M., Fidalgo, C., & Mendez, M. (2022). Functional near-infrared spectroscopy in the neuropsychological assessment of spatial memory: A systematic review. *Acta Psychologica (Amst)*, *224*, 103525. <https://doi.org/10.1016/j.actpsy.2022.103525>

- Lo, F. S., & Erzurumlu, R. S. (2018). Insulin receptor sensitization restores neocortical excitation/inhibition balance in a mouse model of autism. *Molecular Autism*, 9, 13. <https://doi.org/10.1186/s13229-018-0196-6>
- Mansvelder, H. D., Verhoog, M. B., & Goriounova, N. A. (2019). Synaptic plasticity in human cortical circuits: Cellular mechanisms of learning and memory in the human brain? *Current Opinion in Neurobiology*, 54, 186–193. <https://doi.org/10.1016/j.conb.2018.06.013>
- Marks, J. L., Porte, D. Jr., Stahl, W. L., & Baskin, D. G. (1990). Localization of insulin receptor mRNA in rat brain by in situ hybridization. *Endocrinology*, 127(6), 3234–3236. <https://doi.org/10.1210/endo-127-6-3234>
- Masmudi-Martin, M., Navarro-Lobato, I., Lopez-Aranda, M. F., Delgado, G., Martin-Montanez, E., Quiros-Ortega, M. E., Carretero-Rey, M., Narvaez, L., Garcia-Garrido, M. F., Posadas, S., Lopez-Tellez, J. F., Blanco, E., Jimenez-Recuerda, I., Granados-Duran, P., Paez-Rueda, J., Lopez, J. C., & Khan, Z. U. (2019). RGS14(414) Treatment induces memory enhancement and rescues episodic memory deficits. *FASEB Journal*, 33(11), 11804–11820. <https://doi.org/10.1096/fj.201900429RR>
- Mossink, B., et al. (2022). Cadherin-13 is a critical regulator of GABAergic modulation in human stem-cell-derived neuronal networks. *Molecular Psychiatry*, 27(1), 1–18. <https://doi.org/10.1038/s41380-021-01117-x>
- Mueller-Buehl, C., Wegrzyn, D., Bauch, J., & Faissner, A. (2023). Regulation of the E/I-balance by the neural matrixome. *Frontiers in Molecular Neuroscience*, 16, 1102334. <https://doi.org/10.3389/fnmol.2023.1102334>
- Neves, G., Cooke, S. F., & Bliss, T. V. (2008). Synaptic plasticity, memory and the hippocampus: A neural network approach to causality. *Nature Reviews Neuroscience*, 9(1), 65–75. <https://doi.org/10.1038/nrn2303>
- Park, J., Kawai, Y., & Asada, M. (2023). Spike timing-dependent plasticity under imbalanced excitation and inhibition reduces the complexity of neural activity. *Frontiers in Computational Neuroscience*, 17, 1169288–1169288. <https://doi.org/10.3389/fncom.2023.1169288>
- Pelkey, K. A., Chittajallu, R., Craig, M. T., Tricoire, L., Wester, J. C., & McBain, C. J. (2017). Hippocampal GABAergic inhibitory interneurons. *Physiological Reviews*, 97(4), 1619–1747. <https://doi.org/10.1152/physrev.00007.2017>
- Rangel, L. M., Alexander, A. S., Aimone, J. B., Wiles, J., Gage, F. H., Chiba, A. A., & Quinn, L. K. (2014). Temporally selective contextual encoding in the dentate gyrus of the hippocampus. *Nature Communications*, 5(1), 3181. <https://doi.org/10.1038/ncomms4181>
- Rombo, D. M., Ribeiro, J. A., & Sebastiao, A. M. (2016). Hippocampal GABAergic transmission: A new target for adenosine control of excitability. *Journal of Neurochemistry*, 139(6), 1056–1070. <https://doi.org/10.1111/jnc.13872>
- Rubenstein, J. L., & Merzenich, M. M. (2003). Model of autism: Increased ratio of excitation/inhibition in key neural systems. *Genes, Brain, and Behavior*, 2(5), 255–267. <https://doi.org/10.1034/j.1601-183X.2003.00037.x>
- Soto, M., Cai, W., Konishi, M., & Kahn, C. R. (2019). Insulin signaling in the hippocampus and amygdala regulates metabolism and neurobehavior. *Proceedings of the National Academy of Sciences of the United States of America*, 116(13), 6379–6384. <https://doi.org/10.1073/pnas.1817391116>
- Tao, W., Lee, J., Chen, X., Diaz-Alonso, J., Zhou, J., Pleasure, S., & Nicoll, R. A. (2021). Synaptic memory requires CaMKII. *Elife*, 10. <https://doi.org/10.7554/eLife.60360>
- Unger, J., McNeill, T. H., Moxley, R. T. 3rd, White, M., Moss, A., & Livingston, J. N. (1989). Distribution of insulin receptor-like immunoreactivity in the rat forebrain. *Neuroscience*, 31(1), 143–157. [https://doi.org/10.1016/0306-4522\(89\)90036-5](https://doi.org/10.1016/0306-4522(89)90036-5)
- Van Hoeymissen, E., Philippaert, K., Vennekens, R., Vriens, J., & Held, K. (2020). Horizontal hippocampal slices of the mouse brain. *Journal of Visualized Experiments*, 22(163). <https://doi.org/10.3791/61753>
- Wilent, W. B., & Nitz, D. A. (2007). Discrete place fields of hippocampal formation interneurons. *Journal of Neurophysiology*, 97(6), 4152–4161. <https://doi.org/10.1152/jn.01200.2006>
- Wu, F. L., Chen, S. H., Li, J. N., Zhao, L. J., Wu, X. M., Hong, J., Zhu, K. H., Sun, H. X., Shi, S. J., Mao, E., Zang, W. D., Cao, J., Kou, Z. Z., & Li, Y. Q. (2023). Projections from the rostral zona incerta to the thalamic paraventricular nucleus mediate nociceptive neurotransmission in mice. *Metabolites*, 13(2), 226–226. <https://doi.org/10.3390/metabo13020226>
- Yonelinas, A. P., Ranganath, C., Ekstrom, A. D., & Wiltgen, B. J. (2019). A contextual binding theory of episodic memory: Systems consolidation reconsidered. *Nature Reviews Neuroscience*, 20(6), 364–375. <https://doi.org/10.1038/s41583-019-0150-4>

Abbreviations

ASD	autism spectrum disorder
CNS	central nervous system
E/I balance	excitatory/inhibitory balance
EPM	elevated plus maze test
GFP	green fluorescent protein
GAD2	glutamate decarboxylase 2
GABAergic	γ-aminobutyric acidergic
IGF1	insulin-like growth factor 1
InsRs	insulin receptors
IPGTT	intraperitoneal glucose tolerance test
MWM	Morris water maze test
NOR	novel object recognition test
OFT	open field test
PB	phosphate buffer
PBS	phosphate-buffered saline
PBST	phosphate buffered saline with Tween 20
PVDF	polyvinylidene fluoride
rAAV	recombinant adeno-associated virus
Vglut2	vesicular glutamate transporter 2